Roles of RNA silencing-related genes in tomato tolerance to viral infection

(トマトのウイルス感染耐性における

RNA サイレンシング関連遺伝子の役割)

Hokkaido University Graduate School of Agriculture

Division of Agrobiology Doctor Course

Joon Kwon

CONTENTS

LIST OF FIGURES

Chapter 1

Chapter 2

Chapter 3

LIST OF TABLES

GENERAL INTRODUCTION

RNA silencing plays key roles in regulating endogenous gene expression, suppressing transposon activity, silencing transgenes, responding to environmental stimuli and combatting viral infection. In host-virus interactions, RNA silencing triggered by viral double-stranded RNA (dsRNA) is a general antiviral defense mechanism (Ruiz-Ferrer V and Voinnet O 2009). By analogy with the zigzag model that describes plant-microbe interactions, dsRNA and RNA silencing could be regarded as a viral pathogen-associated molecular pattern (PAMP) and PAMP-triggered immunity, respectively (Mandadi KK and Scholthof KB 2013). Most viruses counter the RNA silencing-based antiviral defense by expressing viral suppressors of RNA silencing (VSRs). Therefore, VSRs may be regarded as virulence effectors that facilitate viral infection in plants.

For this reason, research on RNA silencing to virus as a defense mechanism of plants is very important. Tomato (*Solanum lycopersicum* L.; Solanaceae) is susceptible to infection by various plant pathogens. Among the plant viruses that infect tomato, CMV causes extensive economic losses to tomato production (Gallitelli et al, 1988), reducing the number of fruits (69.51–95.65 %) and yield per plant (89.04–99.89 %) (Mahjabeen et al, 2012). In previous studies, host-virus RNA silencing mechamism was reported using model plants (*Nicotiana. benthamiana*, *Arabidopsis. thaliana*, etc.), but there are not many reports in host-virus RNA silencing studies on tomatoes, especially crops.

In this study, roles of RNA silencing in tomato plants was characterized by using two type technology on RNA-mediated interference and genome-editing.

As mentioned before, RNA-mediated interfering technology has a major disadvantage, namely incomplete and unstable inactivation of gene expression. To accomplish complete gene inactivation, several sequence-specifc nucleases, such as zinc-fnger nucleases (ZFNs), transcription activator-like efector nucleases (TALENs) and clustered regularly interspaced short palindromic repeats (CRISPR) systems, have been used in plants (Zhang et al. 2017). Recently,

RNA-dependent DNA cleavage systems, including the CRISPR/Cas9 system, have been frequently used to simplify genome editing in plants (Zhang et al. 2017). The RNA-dependent DNA cleavage systems induce sequence-specific double-strand breaks at sites complementary to the guide RNA sequence, thereby enabling efficient introduction of point mutations, including nucleotide insertions or deletions, to target genes. Recently, Argonaute 2 (AGO2) was inactivated in *N. benthamiana* using the CRISPR/Cas9 system (Ludman et al. 2017). Moreover, infection with the potato virus X vector expressing gfp resulted in higher accumulation of recombinant GFP in the ago2 plants, as compared to that of the WT plants.

In this thesis, focus on elucidating to characterization of RNA-mediated and genome-editing to gene expression and antiviral resistance in tomato plants as three major objectives as follows:

1. RNAi-mediated silencing gene suppression contribute to tolerance of infection with potato virus X and potato virus Y in a susceptible tomato plant.

2. AGO2- and 3-mediated control of systemic necrosis that PVX infection causes in tomato plants.

3. Crispr/Cas9 mediated Inactivation of dicer-like 3 reveals its differential involvement in antiviral responses.

Chapter 1

RNA silencing-related genes contribute to tolerance of infection with potato virus X and Y in a susceptible tomato plant

INTRODUCTION

The plant RNA silencing-based a complex set of proteins to combat intracellular parasites, including viruses, retrotransposons, and other highly repetitive genome elements (Ding SW 2007). This cascade is triggered by double-stranded RNA (dsRNA) or partially double-stranded stem-loop RNA. These are processed by Dicer-like (DCL) nucleases into small RNAs of discrete sizes (21–25 nucleotides [nt]), referred to as small interfering RNAs (siRNAs).

siRNAs are the sequence specificity determinants of RNA-induced silencing complexes (RISC), directing Argonaute (AGO) proteins in RISC to cellular RNA or DNA complementary to the siRNAs. This process silences corresponding genes or genetic elements through targeted cleavage, repression of translation, or DNA methylation (Calarco et al 2011, Chen 2010). In some eukaryotes, such as plants and fungi, cellular RNA-dependent RNA polymerase (RDR) acts to convert aberrant RNAs to dsRNA, leading to small RNA amplification and more intensive RNA silencing (Cogoni et al 1999, Dalmay et al 2000, Wang et al 2010).

RNA viruses produce dsRNA as a replication intermediate, thus rendering them targets of RNA silencing (Xie Z et al 2004). DCL2 and DCL4 are largely responsible for processing viral dsRNAs into small pieces, termed virus-derived siRNAs (vsiRNAs), which can then be incorporated into RISC (Bouché et al 2006, Andika et al 2015, Brosseau et al 2015, Deleris et al 2006, Diaz-Pendon et al 2007, Dunoyer et al 2007, Garcia-Ruiz et al 2015, Qu et al 2008). The resulting "aberrant" viral RNA cleavage products are thought to be substrates for plant RDR proteins, which subsequently generate more dsRNA (Wang et al 2010). The major contributors to the production of secondary vsiRNAs are RDR1, RDR2, and RDR6 (Zhang et al 2015). In an *in vitro* assay, *Arabidopsis* AGO1, AGO2, AGO3, and AGO5 showed antivirus activity against a member of the genus *Tombusvirus*. In addition, specific AGOs (e.g., AGO1, AGO2, AGO3, AGO4, AGO5, and AGO9) were shown to selectively bind small RNAs derived from viroids or viruses (Minoia et al 2014, Schucket al 2013, Takeda et al 2008, Wang et al 2011). These results suggest that

multiple AGO proteins have the intrinsic ability to target viruses. Several AGO mutants were shown to increase susceptibility to viruses (Carbonell et al 2015), examples include AGO1 mutants and cucumber mosaic virus (CMV), turnip crinkle virus (TCV), and brome mosaic virus (Qu et al 2008, Harvey et al 2011, Jaubert et al 2011, Ma et al 2015); AGO4 mutants and tobacco rattle virus (Odokonyero et al 2015, Fernández-Calvino et al 2016); and an AGO7 mutant and TCV (Qu F et al 2008). Among them, AGO2 appears to be a major player in RNA silencing against viruses and has been implicated in defense against CMV, TCV, tobacco rattle virus, potato virus X (PVX), turnip mosaic virus (TuMV), and tomato bushy stunt virus (Zhang et al 2015, Wang et al 2011, Carbonell et al 2015, Harvey et al 2011, Jaubert et al 2011, Ma et al 2015, Odokonyero et al 2015, Fernández-Calvino et al 2016, Scholthof et al 2015). In addition, AGO5 appears to play a secondary antiviral role in the absence of AGO2 (Brosseau et al 2015, Garcia-Ruiz et al 2015). Meanwhile, attenuated viruses with mutated virus silencing suppressors have also been used to identify plant factors involved in antiviral silencing, including DCL2, DCL4, AGO1, AGO2, DRB4, RDR1, RDR6, and HEN1 (Wang et al 2010, Diaz-Pendon et al 2007, Wang et al 2010, Wang et al 2011, Scholthof et al 2015).

Potato virus X is a type member of the genus *Potexvirus* (Alphaflexiviridae). PVX predominantly infects *Solanaceous* plants. Recent studies employing *A. thaliana* revealed that RNA silencing is the chief determinant of the non-host immunity against PVX. Indeed, inactivation of DCLs (DCL2 and DCL4) or AGO2 enable PVX to efficiently infect *A. thaliana* plants (Andika et al 2015, Harvey et al 2011, Andika et al 2015). Another study demonstrated that the full restriction of PVX requires AGO5 in addition to AGO2 (Brosseau et al 2015).

Potato virus Y is a type member of the genus *Potyvirus*, family *Potyviridae* (Plisson et al 2003). Potato virus Y (PVY) is a flexuous rod-shaped virus; its genome consists of a single-strand positive sense RNA (length: ~9.7 kb), which contains two opening reading frames (ORFs) encoding 12 proteins. In PVY ORFs, two proteins (P3N-PIPO and P3N-ALT) are expressed

through the RNA polymerase slippage mechanism in the P3 cistron (Karasev et al 2013, Riechmann et al 1992, Chung et al 2008, Olspert et al 2015, Wylie et al 2017, Komoda et al 2016).

Tomato (*Solanum lycopersicum*) is an important vegetable crop and a model plant for the research of fruit development and plant defense (Bergougnoux et al 2014). There are 7 DCLs, 15 AGOs and 6 RDRs encoded in the tomato genome (Bai M et al 2012). An analysis of tomato DCL1 and DCL3-silencing mutants indicates that DCL1 produces canonical miRNAs and a few 21-nt siRNAs (Kravchik et al 2014) and DCL3 is involved in the biosynthesis of heterochromatic 24-nt siRNAs and long miRNAs (Kravchik et al 2014). DCL4 is required for the production of 21-nt tasiRNAs that in turn target the ADP-ribosylation factors (ARFs) to alter tomato leaf development (Yifhar et al 2012). Extended number of the DCL2 genes, i.e., DCL2a, DCL2b, DCL2c, and DCL2d, are encoded in tomato (Bai et al 2012). Recently, DCL2b dependent miRNA pathway in tomato affects susceptibility to PVX and TMV (Wang et al 2018) also DCL2b is also required for the biosynthesis of 22-nt small RNAs to defense against ToMV (Wang et al 2018).

In this study, the virulence of PVX and PVY were examined in transgenic tomato plants, in which the expression of the DCL2, DCL4, AGO2, AGO3 and RDR6 genes was suppressed. The goal of this study is to investigate whether these RNA silencing-related genes are involved in tolerance or defense to infection with these viruses in tomato plants

MATERIAL AND METHODS

Plants and viruses

Wild-type tomato (*Solanum lycopersicum* cv. Moneymaker) and transgenic tomato plants created from Moneymaker were used in this study. DCL2 and DCL4- and RDR6-repressed (hpDCL2.4 and hpRDR6) tomato plants were described in the previous studies (Suzuki et al 2019, Naoi et al 2020). Tomato plants AGO2a, AGO2b and AGO3 (Solyc02G069260, Solyc02G069270, and Solyc02G096280, registered in the tomato genome database at https://solgenomics.net/organism/Solanum_lycopersicum/genome) are repressed (hpAGO2.3) were created in the same manner as hpDCL2.4 tomato plants (Suzuki et al 2019). The inverted repeat (IR) sequences were constructed by placing parts of AGO2, AGO3 (947 bp) in a head-to-head orientation across an intron sequence to create an IR sequence (Fig 1-1). In addition, tomato plants transformed with pIG121-Hm containing an empty cassette were created and used as a negative control (empty vector). PVX derived from the infectious clone pP2C2S, which was constructed with the PVX-UK3 strain (Chapman S et al., 1992), as well as the N (Ohki T et al., 2018) and O (Masuta C et al., 1999) strains of PVY (PVY^N and PVY^O) were used for the inoculation tests in this study.

Plant growth conditions and viral infection

Tomato plants were cultivated in a growth room at 21–23°C with a 16-h photoperiod. PVX- and PVY-infected leaf discs (50 mg) were ground in inoculation buffer (0.1 M phosphate buffer [pH 7.0], 1% 2-mercaptoethanol). The crude sap was mechanically inoculated onto the first and second leaves of 2-weeks old tomato plants. At the same time, other plants were inoculated with inoculation buffer alone as a control (mock inoculation).

Reverse transcription-polymerase chain reaction (RT-PCR) and real-time PCR

PVY genomic RNA was detected using RT-PCR as follows. Tomato leaves were ground in liquid nitrogen, and total RNA was extracted with TRIzol™ Reagent (Thermo Fisher Scientific, Inc., Waltham, MA, USA). All RNA samples were treated with RNase-free DNase I (Roche Diagnostics, Basel, Switzerland). cDNA was synthesized from 1 μg of RNA extract using the modified Moloney Murine Leukemia Virus (MMLV) reverse transcriptase ReverTra Ace® (Toyobo, Osaka, Japan). PCR was performed to detect viral genomic RNA and endogenous mRNA. The mixture (25 μl) contained cDNA corresponding to 0.1 μg RNA, 0.4 μM of each of the specific primer pairs. 0.2 mM deoxyribonucleotide triphosphate (dNTPs), and 0.625 U Ex Taq™ DNA polymerase (Takara, Otsu, Siga, Japan). PCR mixtures were incubated for 2 min at 94°C, followed by 28 cycles at 94°C for 30 s, 60°C for 30 s, and 72°C for 60 s. The PCR products were fractionated through 1.2% agarose gel electrophoresis. Quantitative PCR (qPCR) was performed using the AriaMx real-time PCR system (Agilent Technologies, Santa Clara, CA, USA). The reaction mixture (25 μl) contained 0.3 mM (each) forward and reverse primers (Additional file 1: Table S1), 0.2 mM dNTPs, 0.625 U Ex Taq™ DNA polymerase (Takara), SYBR Green (1/800 dilution) (Thermo Fisher Scientific), and cDNA obtained by reverse transcribing 50 ng of total RNA. Samples were incubated for 2 min at 95°C, followed by 39 cycles at 95°C for 10 s, and at 58°C and 72°C for 20 s each.

Northern and western blotting assays

Accumulation of the PVX CP and PVY CP and these genomic RNAs was investigated through western and northern blotting as previously described (Jeon EJ et al., 2017). Upper uninoculated leaves from each plant at each different days post-inoculation (dpi) were harvested and total RNA preparations (1–10 μg) were extracted using TRIzol™ Reagent (Thermo Fisher Scientific). Following transfer to a nylon membrane (Hybond-N; GE Healthcare, Chicago, IL, USA), hybridization with a digoxigenin-labeled probe (Roche Diagnostics) was performed to detect the 3′-terminal regions of the genome segments. Chemiluminescence signals with CDP-star (Millipore Sigma, St. Louis, MO, USA) were quantitatively detected using a LAS-4000 mini-imaging system (GE Healthcare).

Western blotting was conducted as previously described (Nakahara et al 2012). Total proteins were separated through electrophoresis in 12% sodium dodecyl sulfate-polyacrylamide (SDS) gel electrophoresis and transferred onto nylon membrane. For the detection of viral coat proteins, primary antibodies raised against PVX CP and PVY CP, provided by Japan Plant Protection Association, were used at a 1:1000 dilution, while alkaline phosphatase-conjugated goat antirabbit immunoglobulin G (Thermo Fisher Scientific) was used as the secondary antibody. Chemiluminescence signals were detected using the CDP-Star reagent in a LAS-4000 mini-imaging system.

RESULTS

DCL2, DCL4 and AGO2 are involved in tolerance to PVX infections in tomato

Repression of the expression levels of mRNAs confirmed in hpDCL2.4, hpAGO2.3, and hpRDR6 plants by real-time RT-PCR. The expression levels of DCL2a, b, c and DCL4 were also decreased to approximately 3%, 10%, 8% and 15%, respectively, in transgenic tomato plants compared with empty vector transformed plants (Figure1-1). In hpAGO2.3 and hpRDR6 plants, the expression levels of both AGO2b and RDR6 genes were decreased to approximately 29% and 36% of the wild-type levels. In contrast, the expression levels of the DCL2d, AGO2a and b were not altered significantly in hpDCL2.4 and hpAGO2.3 plants.

These transgenic tomato plants inoculated with PVX were observed non-inoculated upper leaves of all inoculated plants at 5 dpi (Figure1-2, Table 1). The symptoms that developed in hpDCL2.4 and hpAGO2.3 were more severe symptoms and the control transgenic plants with the empty vector. Specifically, necrotic spots developed in hpAGO2.3 plants on the upper leaves at 5 dpi, and the necrotic symptoms spread systemically at 20 dpi (Figure 1-2). More severe dwarfing, as well as mosaics and leaf-malformation were observed in the hpDCL2.4 plants (Figure1-2).

The accumulation of PVX CP and the genomic RNAs with investigated with blotting assays (Figure 1-3) to confirm whether the difference in symptom was associated with the multiplication of PVX in these plants. The three transgenic tomato the empty vector (Empty) control plants all accumulated CP and the full-length genomic RNA at 15 day post inoculation (dpi) (Figure 1-3). Of note, the accumulation of subgenomic RNAs differed among the samples. The levels of DCLs, AGOs and RDR6 mRNAs in transgenic lines infected with PVX were investigated by RT-qPCR (Figure 3-1). The levels of DCL2a, DCL2c and DCL4 mRNAs in hpDCL2.4 lines infected with PVX were lower than those in the healthy empty vector-transformed plants.

Also, the mRNA levels of DCL2(a,b,c) and DCL4 were also reduced in the PVX-infected empty vector-transformed plants. In contrast, the mRNA levels of DCL2b and DCL2d were increased in the PVX-infected hpDCL2.4 and empty vector-transformed plants (Figure 1-3). In hpAGO2.3 and hpRDR6 plants infected with PVX, the mRNA levels of AGO2, AGO3 and RDR6 were similar to those in the PVX-infected and healthy empty vector-transformed plants (Figure 1-3).

Table 1-1 Reaction of transgenic plants following mechanical inoculation with PVX-UK3 and PVY^N strains

Host plants	Symptoms on leaves*			
	5 dpi	10 dpi	15 dpi	20 dpi
PVX-inoculated				
hpDCL2.4	-/M, Mal	-/M, Mal	-/M, Mal	-/M, Mal
hpRDR6	-/M	-/M	-/M	-/M
hpAGO2.3	-/M, NS	-/M, NS	-/M, NS	-/M, NS
Empty	-/M	-/M	-/M	-/M
Mock	-/-	-/-	-/-	-/-
PVY^N-inoculated				
hpDCL2.4	-/-	-/-	-/mM, Mal	-/M, Lc
hpRDR6	-/-	-/-	-/-	-/-
hpAGO2.3	-/-	-/-	-/-	-/-
Empty	-/-	-/-	-/-	-/-
Mock	-/-	-/-	-/-	-/-

A

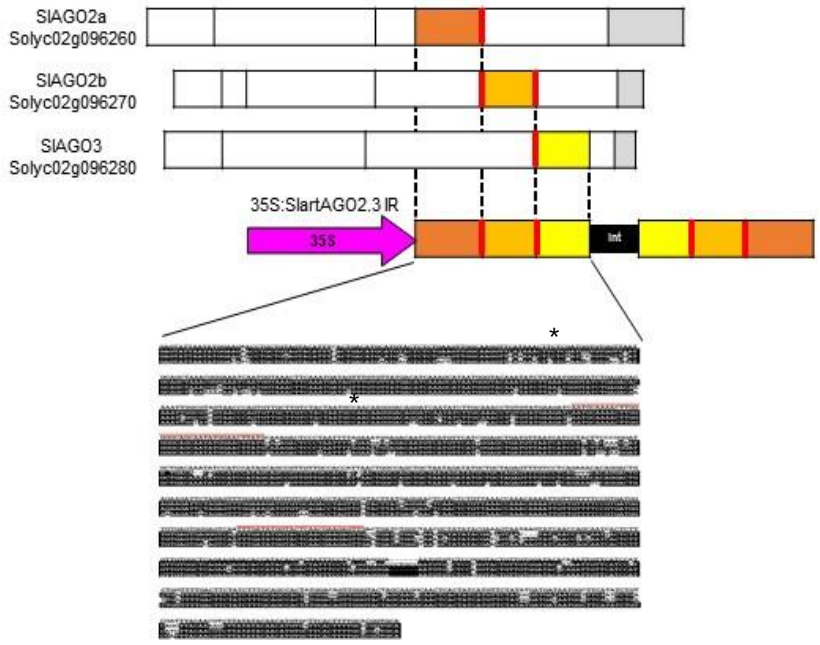
SlAGO2a
Solyc02g096260
SlAGO2b
Solyc02g096270
SlAGO3
Solyc02g096280
35S:SlartAGO2.3 IR
35S
int
*
*

B

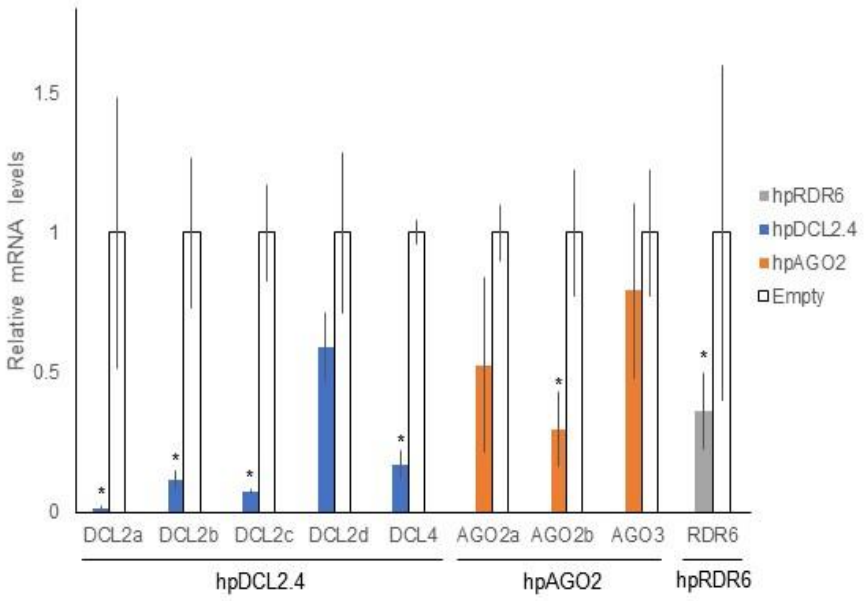
Relative mRNA levels
1.5
1
0.5
0
hpRDR6
hpDCL2.4
hpAGO2
Empty
DCL2a
DCL2b
DCL2c
DCL2d
DCL4
AGO2a
AGO2b
AGO3
RDR6
hpDCL2.4
hpAGO2
hpRDR6

Figure 1-1 Schematic diagram of the artificial chimera gene (SlAGO2 and 3) and Relative expression levels of the DCLs, AGO2, and RDR6 mRNAs in transgenic *S. lycopersicum*

(A) Based on the alignment of two tomato AGO genes (SlAGO2a, b and SlAGO3) sequences registered in the database, three regions from SlAGO, i.e., as shown in the top of the figure. (B) The relative levels of these mRNAs were investigated through real-time reverse transcription-polymerase chain reaction (RT-PCR) using the 18S ribosome RNA as a control. Error bars represent SE. Student's t-test was applied to analyze the data, comparing the dsRNA-expressing and empty vector-transformed plants. Asterisks indicate a statistically significant difference in mRNA accumulation of the gene between plants with/without expressing dsRNA ($P<0.05$).

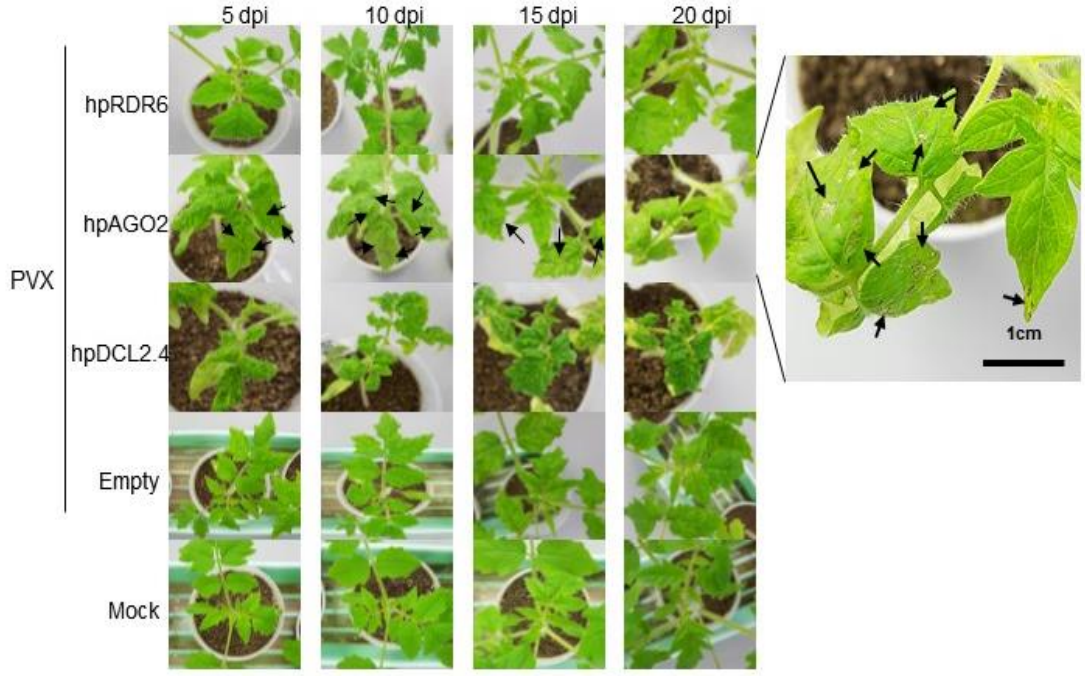

Figure 1-2 Symptoms developed in hpRDR6, hpAGO2.3, and hpDCL2.4 transgenic tomato plants inoculated with PVX. Photographs were captured at 5, 10, 15, and 20 days-post-inoculation (dpi). The empty vector-transformed Moneymaker tomato plants were also inoculated with PVX (Empty) and buffer (Mock) as controls.

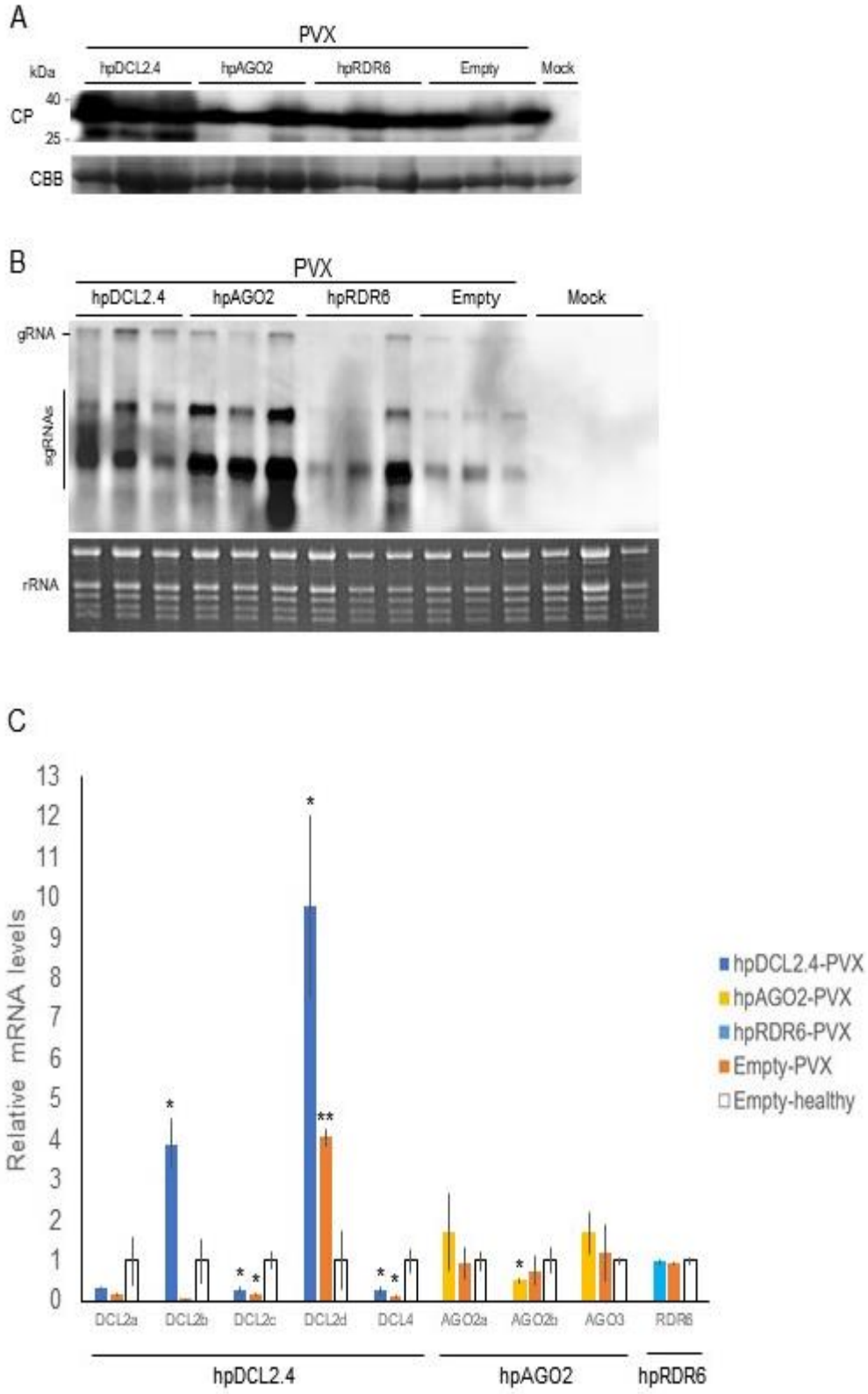
A
PVX
kDa
hpDCL2.4
hpAGO2
hpRDR6
Empty
Mock
40
25
CP
CBB
B
PVX
hpDCL2.4
hpAGO2
hpRDR6
Empty
Mock
gRNA
sgRNAs
rRNA
C
Relative mRNA levels
13
12
11
10
9
8
7
6
5
4
3
2
1
0
DCL2a
DCL2b
DCL2c
DCL2d
DCL4
AGO2a
AGO2b
AGO3
RDR6
hpDCL2.4
hpAGO2
hpRDR6
hpDCL2.4-PVX
hpAGO2-PVX
hpRDR6-PVX
Empty-PVX
Empty-healthy

Figure 1-3 Detection of PVX CP and genomic RNA in tomato plants inoculated with PVX using western (A) northern blotting (B) and qRT-PCR (C). (A) Total protein samples were prepared from non-inoculated upper leaves of tomato plants (hpRDR6, hpAGO2.3, and hpDCL4.2) at 15 dpi. The coomassie brilliant blue-stained gel was used as a loading control (CBB). (B) Total RNAs extracted from hpRDR6, hpAGO2.3, hpDCL2.4, Empty, and Mock plants at 15 dpi were to detect the PVX genomic (gRNA) and subgenomic RNAs (sgRNAs) in non-inoculated upper leaves through northern blotting. rRNA was used as a loading control. (C) RT-qPCR to compare the mRNAs level in the upper leaves of hpDCL2.4, hpAGO2.3, hpRDR6 and empty vector-plants infected with PVX (Empty-PVX) with that in the healthy empty vector plants (Empty-healthy) at 15 dpi. 18S ribosome RNA was used are control. Error bars represent SE. Student's t-test was applied to analyze the data. The values with the double asterisk (**; $p < 0.01$) and single asterisk (*; $p < 0.05$) were statistically significant at 1% and 5% levels, compared to those of Empty-healthy.

DCL2 and DCL4 were required for defense against infection with PVY

For mechanically-inoculated PVY^N onto hpDCL2.4, hpAGO2.3, and hpRDR6 plants, symptoms were only observed on the non-inoculated upper leaves of hpDCL2.4 (Fig. 1-4, Table 1-1). PVY^N CP and its genomic RNA were detected by western blotting and RT-PCR. PVY CP was detected via western blotting only in DCL2.4 plants, which exclusively showed symptoms (Fig 1-5). PVY genomic RNA was detected through semi-quantitative RT-PCR in all the inoculated plants at 15 dpi under 30 cycles of amplification. However, after 20 cycles of amplification, it was detected only in hpDCL2.4 plants (Fig 1-5). In RT-qPCR analysis, detected a reduction in mRNA levels in all of to the tested genes in PVY^N-infected hpDCL2.4, hpAGO2.3 and hpRDR6 plants compared with PVY^N-infected empty vector-transformed plants. In contrast, the mRNA levels of DCL2d, AGO2a and RDR6 in the PVY-infected empty vector-transformed plants were lower than those in the PVY-infected hpDCL2.4, hpAGO2.3 and hpRDR6 plants.

The parental cultivar and hpDCL2.4 plants were inoculated with both PVY^N and PVY^O, and compared their susceptibility to the viruses (Table 1-2). This experiment was performed to rule out the possibility that stresses during the production of transgenic plants affect their susceptibility to PVY^N and PVY^O in a strain-specific manner. As expected, the hpDCL2.4 plants inoculated with both strains showed symptoms; however, none of the inoculated parental cultivar plants developed symptoms (Table 1-2). In addition, PVY CP was detected using western blotting only in hpDCL2.4 plants inoculated with both PVYs (Fig 1-6) though PVY CP was observed in the PVY-inoculated Moneymaker cultivar at 40dpi (Fig 1-6). PVY genomic RNA was detected in all the samples from both PVY-inoculated plants by RT-PCR at 20 dpi and in the following days. However, at 15 dpi, PVY genomic RNA was detected only in the samples obtained from hpDCL2.4 (Fig 1-6). These results indicate that PVY latently and systemically infects the Moneymaker cultivar. Moreover, silencing of DCL2 and DCL4 increases the accumulation of PVY CP and its genomic RNA, resulting in the development of symptoms.

Table 1-2. Reactions of transgenic plants following mechanical inoculation with PVY^N and PVY^O strains

Host plants	Symptoms on leaves*			
	5 dpi	10 dpi	15 dpi	20 dpi
PVY^N-inoculated				
hpDCL2.4	-/-	-/-	-/mM, Mol	-/mM, Mol
Moneymaker	-/-	-/-	-/-	-/-
Healthy control	-/-	-/-	-/-	-/-
PVY^O-inoculated				
hpDCL2.4	-/mM, Mol	-/mM, Mol	-/mM, Mol	-/mM, Mol
Moneymaker	-/-	-/-	-/-	-/-
Healthy control	-/-	-/-	-/-	-/-

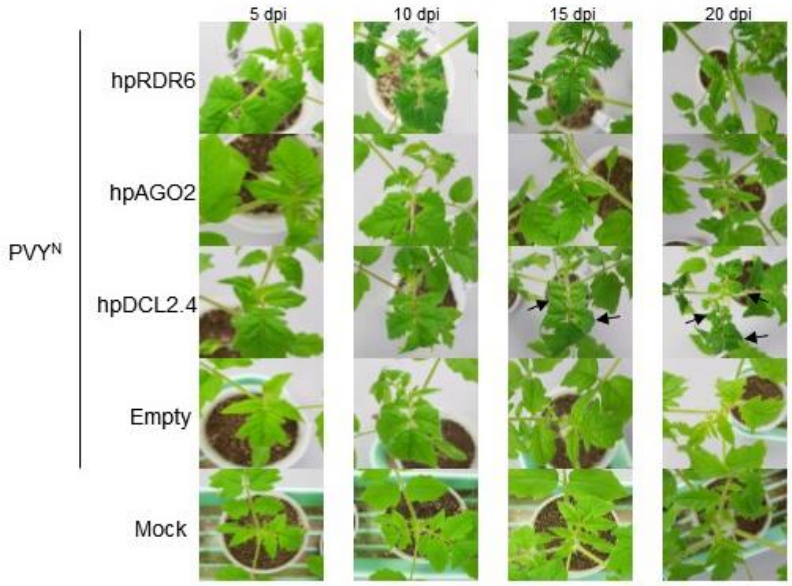

Fig 1-4 Symptoms developed in hpRDR6, hpAGO2.3, and hpDCL2.4 transgenic tomato plants inoculated with PVY^N. Photographs were captured at 5, 10, 15, and 20 dpi. The empty vector-transformed Moneymaker tomato plants were also inoculated with PVY^N (Empty) and buffer (Mock) as controls.

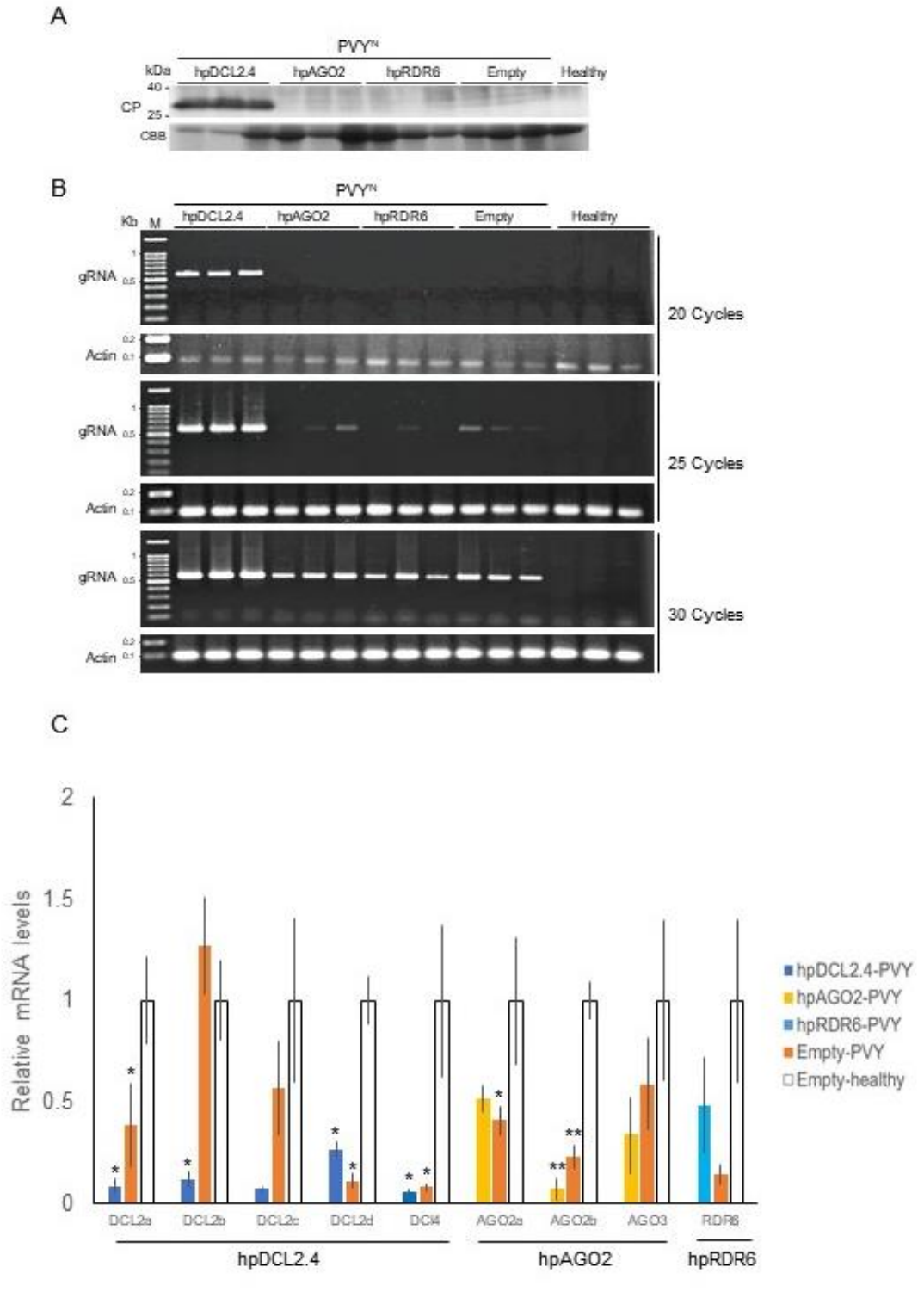
A
PVY^N
kDa
hpDCL2.4
hpAGO2
hpRDR6
Empty
Healthy
40 -
CP
25 -
CBB
B
PVY^N
Kb
M
hpDCL2.4
hpAGO2
hpRDR6
Empty
Healthy
gRNA
Actin
20 Cycles
25 Cycles
30 Cycles
C
Relative mRNA levels
2
1.5
1
0.5
0
DCL2a
DCL2b
DCL2c
DCL2d
DCl4
AGO2a
AGO2b
AGO3
RDR6
hpDCL2.4
hpAGO2
hpRDR6
hpDCL2.4-PVY
hpAGO2-PVY
hpRDR6-PVY
Empty-PVY
Empty-healthy

Fig 1-5 Detection of viral CP and genomic RNA (gRNA) in tomato plants inoculated with PVY^N. (A) For the detection of CP, total protein was extracted from the upper leaves of tomato plants (hpRDR6, hpAGO2.3, and hpDCL4.2) at 15 dpi. The CBB-stained gel was used as a loading control. (B) Semi-quantitative RT-PCR for the levels of PVY^N genomic RNA in non-inoculated upper leaves of tomato plants at 15 dpi. Their PCR products at 20, 25, and 30 cycles were fractionated using agarose gels. The actin gene was used as a control. (C) RT-qPCR to compare the mRNAs in the upper leaves of transgenic tomato plants and empty vector transformed plants infected with PVY^N (Empty-PVY) with that in the healthy empty vector plants (Empty-healthy) at 15 dpi. 18S ribosome RNA as used control. Error bars represent SE. Student's t-test was applied to analyze the data. Each analysis was done with three biological replicates. The values with the double asterisk (**; $p < 0.01$) and single asterisk (*; $p < 0.05$) were statistically significant at 1% and 5% levels, compared to those of healthy Empty-healthy.

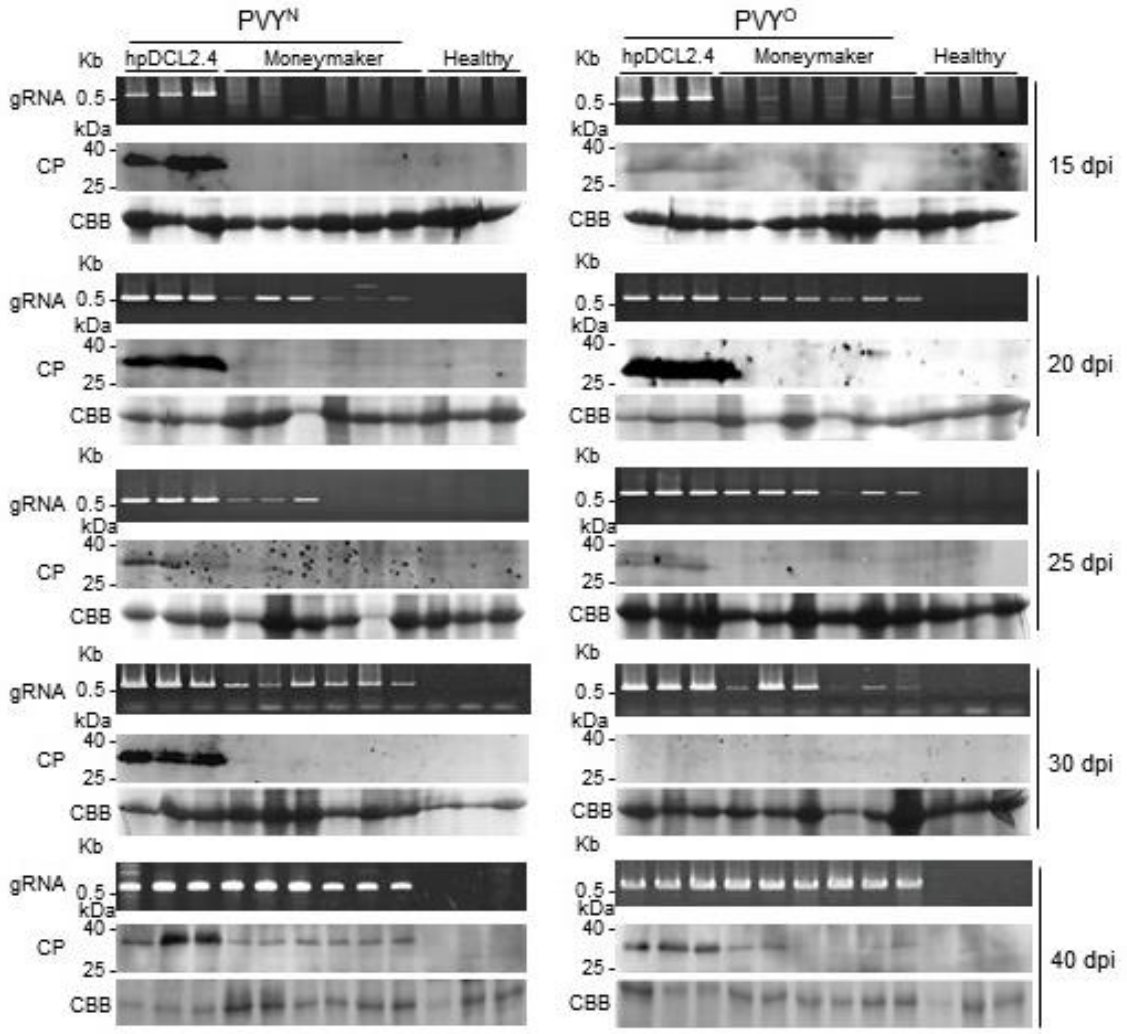

Fig 1-6 Time course analysis of PVY CP and genomic RNA (gRNA) levels in upper leaves of hpDCL2.4 and the parental cultivar Moneymaker. Non-inoculated Moneymaker plants were analyzed as a control (Healthy). Total RNA and protein were extracted from the leaves of these plants at 15, 20, 25, and 30 dpi. M is the 100 bp DNA ladder. CBB-stained gels were used as a loading control (RUBISCO protein).

DISCUSSION

Silencing the DCL and AGO genes altered the reactions of a susceptible tomato plant to infection with PVX and PVY. The symptoms on PVX infection were exacerbated in DCL2, DCL4, AGO2 and AGO3-knockdown transgenic tomato plants. Severe dwarfing and leaf deformation observed in hpDCL2.4 and more severe mosaics in hpDCL2.4 and necrotic systems in hpAGO2.3 plants were observed compared to those in the PVX-inoculated other transgenic and wild-type plants. On the other hand, infection with PVY caused symptoms only in hpDCL2.4-knockdown plants, but not in the other transgenic or wild-type plants. RT-PCR tests showed that all PVY-inoculated plants were systemically infected with PVY, indicating that the tomato cultivar 'Moneymaker' is susceptible to infection with PVX and PVY. These results suggest that DCL2, DCL4, AGO2 and AGO3 are involved in tolerance to infection with PVX and PVY in a susceptible tomato plant. Considering that significantly increased levels of the DCL2b and DCL2d mRNAs in the PVX-infected hpDCL2.4 plants, severer symptoms are not necessarily caused by downregulation of the DCL genes.

DCL2, DCL4, AGO2 and AGO3 are important factors in the RNA silencing-mediated antiviral defense (Diaz-Pendon et al 2007, Qu et al 2008, Wang et al 2011, Scholthof et al 2010, Riechmann et al 1992, Vazquez et al 2006). This would be the case for the tolerance to infection of two strains of PVY (i.e., PVY^N and PVY^O), involving DCL2 and DCL4. Western blotting was only able to detect PVY CP in the inoculated hpDCL2.4 plants though it also detected PVY CP in the inoculated moneymaker plants at 40 dpi. RT-PCR consistently detected PVY genomic RNA in the lower PCR cycle numbers and time-course experiments in samples from the inoculated hpDCL2.4 plants, although all inoculated plants were systemically infected with PVY. There results indicate that the higher accumulation of PVY in the hpDCL2.4 plants is probably attributed to the reduced activity of RNA silencing against PVY. DCL proteins possess RNase III activity

to generate small RNAs, such as siRNAs and microRNAs (miRNAs) (Vazquez F et al 2006), and silencing or mutations in DCLs would affect siRNA biogenesis.

A recently study showed a defect in the biogenesis of siRNAs, especially 22 nt siRNAs, derived from viroid RNA in the hpDCL2.4 plants infected with the potato spindle tuber viroid (Suzuki et al 2019). Other studies have reported the increased accumulation of TuMV and CMV genomic RNAs in DCL2- and DCL4-knockdown *N. benthamiana* (Garcia-Ruiz et al 2010, Matsuo et al 2017). Silencing of DCL4 facilitates the systemic movement of zucchini yellow mosaic virus in *N. benthamiana* (Cordero et al 2017). These studies indicate that DCL2 and DCL4 restrict the multiplication of viruses in susceptible plants. In this study, tomato DCL2 and DCL4 also did not completely prevent infection with PVY. However, they efficiently restricted infection to reduce the occurrence of symptoms in a susceptible cultivar.

PVX has a relatively weak RNA silencing suppressor, triple gene block protein 1 (TGBp1) (Senshu et al 2009), and may have the ability to escape or survive under active conditions of antiviral RNA silencing (Van Wezel et al 2004). This ability may partly explain the absence of an obvious increase in PVX accumulation in DCL2.4 and AGO2 plants. RNA silencing is one of the major antiviral defence mechanisms involved in the regulation of numerous endogenous genes via siRNAs and miRNAs (Csorba et al 2009). Thus, symptom exacerbations may be attributed to differences in the expression of the endogenous genes via the knockdown of DCL2, DCL4, AGO2 and AGO3. A previous study showed that the symptom exacerbations in hpDCL2.4 plants infected with potato spindle tuber viroid could be attributed to the increased expression of miR398a-3p, which increased the production of reactive oxygen species (Wang et al 2018).

Similar symptom exacerbations, including systemic necrosis, have been observed in the AGO2-knockout *N. benthamiana* using CRISPR/Cas9 (Ludman et al 2017). The *Arabidopsis* Col-0 plant is a non-host for PVX; however, PVX becomes capable of multiplication in the inoculated leaves in the AGO2 mutant (Jaubert et al 2011). P25, also known as triple gene block protein 1 (TGBp1),

suppresses RNA silencing (Verchot-Lubicz et al 2007, Voinnet et al 2000), which can be partly explained by P25 is binding to AGO1 and directing the degradation of AGO1 via the 26S proteasome (Cho et al 2016). Also, P25 has an affinity for AGO2 (Jaubert M et al 2011). Necrosis or cell death associated with PVX infection or closely related viruses that belong to the genus *Potexvirus* has been reported. Infection with PVX triggers hypersensitive cell death responses in potato plants carrying the Nb gene, and P25 is the elicitor of these responses (Malcuit et al 1999). TGBp3 induces the unfolded protein response during PVX infection. This effect is important in the regulation of cellular cytotoxicity that could otherwise lead to cell death if the viral proteins reach high levels in the ER (Ye et al 2011, Lu et al 2016). An isolate of the plantago asiatica mosaic virus causes systemic necrosis in *N. benthamiana*, and its RNA-dependent RNA polymerase is a virulence determinant for necrotic symptoms (Ozeki et al 2006). Isolate of the PVX-OS strain induced systemic necrotic mosaic in *Nicotiana* spp. and its 1422 amino acid in C-terminal of RNA-dependent RNA polymerase is a determinant for systemic necrotic mosaic symptoms (Kagiwada et al 2005). Co-infection with PVX and PVY causes systemic necrosis in tobacco plants, and PVX P25 and PVY helper component-protease have been identified as determinants for necrotic symptoms (Pacheco et al 2012). Downregulation of double-stranded-RNA-Binding Protein (DRB2) by VIGS is able to reduce PVX-triggered systemic necrosis in ago2 mutant *N. benthamiana* (Fátyol et al 2020).

These previous studies may help reveal the mechanism through which AGO2-knockdown alters the expression of endogenous genes and which host and viral genes involved in the development of necrotic symptoms during infection with PVX.

Chapter 2

Molecular mechanisms underlying AGO2- and AGO3-mediated control of systemic necrosis that PVX infection causes in tomato

INTRODUCTION

In host-virus interactions, RNA silencing triggered by viral double-stranded RNA (dsRNA) is a general mechanism involved in immunity against viruses (Ruiz-Ferrer et al 2009). By analogy with the zigzag model that describes plant-microbe interactions, dsRNA and RNA silencing could be regarded as a viral pathogen-associated molecular pattern (PAMP) and PAMP-triggered immunity, respectively (Mandadi et al 2013). Most viruses counter the RNA silencing-based antiviral defense by expressing viral suppressors of RNA silencing (VSRs). Therefore, VSRs may be regarded as virulence effectors that facilitate viral infection in plants. As suggested by the zigzag model, plants may have developed a countermeasure against viral VSRs through the recognition of these viral effectors as avirulence (avr) factors to induce resistance (R) gene-mediated resistance. Indeed, VSRs are recognized by R genes to trigger immune responses. For example, the Cauliflower mosaic virus VSR protein P6 is an avr determinant recognized by R genes in several plants (Király et al 1999, Love et al 2007). Similarly, the Tomato bushy stunt virus (TBSV) P19 silencing suppressor is also an elicitor of hypersensitive response (HR) in certain *Nicotiana* species (Angel et al 2013).

Potato virus X (PVX), a positive-sense single-stranded RNA virus, belongs to the genus *Potexvirus* and its genome carries replicase gene comprising methyltransferase (MET), helicase (HEL), and polymerase (POL) motifs, a triple gene block (TGB) encoding TGB1, TGB2, and TGB3, involved in viral movement and silencing suppression, and a coat protein (CP) which has a structural role as well as being a silencing suppressor and necessary for viral movement (Wong et al 1997).

In response to pathogen infection, plants induce two layers of defense responses called pathogen associated molecular patterns (PAMPs)-triggered immunity (PTI) and effector-triggered immunity that involve the activation of various plant defense responses, including programmed cell death (De et al 2018). Also, reactive oxygen species (ROS) and that ROS play a central role in plant immune responses pathway (Lamb and Dixon et al 1997, Doke 1983) ROS are toxic to

plant cells at high concentrations and thus must be maintained at appropriate levels by a delicate balance between ROS-producing and -scavenging enzymes (Mittler et al 2004, Miller et al 2010). Major ROS scavenging enzymes include ascorbate peroxidase (APX1), catalase (CAT1 and 2), thylakoid aperoxidase (tAPX), mitochondrial oxidase (AOX) and Cu-Zn-superoxide dismutase 2 (CSD2) (Mittler et al 2004).

Systemic necrosis is one of the most severe symptoms caused by plant viruses, which eventually leads to cell death in virus-infected systemic leaves (Syller 2012). In several compatible pathosystems, systemic necrosis has been shown to share biochemical, physiological and molecular features with the hypersensitive response (HR), a form of PCD (García-Marcos et al 2013, Komatsu et al 2010, Mandadi and Scholthof 2013) Co-infection, but not single infection, of *N. benthamiana* plants with PVX and several members of the Potyvirus genus results in systemic necrosis, which correlates with the transcriptional activation of defence-related genes and PCD(García-Marcos et al 2013, García-Marcos et al 2009). Contrary to that which has been observed in other PVX-associated synergisms (De et al 2018, Vance 1991), the levels of PVX gRNA were not substantially increased in *N. benthamiana* plants when doubly infected with PVX and either Plum pox virus (PPV), Potato virus Y (PVY) or Tobacco etch virus (TEV), despite the synergism in pathology that leads to extreme augmentation of symptoms in this host (González-Jara et al 2005, González-Jara et al 2004). Previous data showed that Agrobacterium-mediated transient co-expression of PVX together with viral suppressors of RNA silencing (VSRs) recapitulated in local tissues the systemic necrosis caused by PVX–potyvirus synergistic infections (Aguilar et al 2015). Moreover, ectopic expression of the potexviral P25 (TGB1) protein encoded by the TGB subgenomic RNA (sgRNA) was sufficient to elicit a cell death response when overexpressed with other VSRs, including the helper component-proteinase (HC-Pro) protein of potyvirus (Aguilar et al 2015). A frameshift mutation in the P25 open reading frame (ORF) of PVX, which maintained unaltered the TGB3 gene, did not lead to necrosis when co-expressed with VSRs, suggesting that P25 is the main PVX determinant involved in the

elicitation of a systemic HR-like response in PVX-associated synergisms. Synergy is often manifested by a remarkable increase in both virus accumulation and symptom expression, compared to single infections (Aguilar et al 2015). The best studied synergistic interaction involves Potato virus X (PVX) with a number of potyviruses in tobacco (*Nicotiana* spp.) plants, in which the level of PVX is enhanced severalfold compared to its level in singly infected plants (Pruss et al 1997, Vance et al 1995). Potyvirus-associated synergistic diseases have been suggested to result from suppression of the host defense mechanism based on RNA silencing by the potyviral VSR, helper component-proteinase (HC) protein (Pruss et al 1997). However, the accumulation of PVX genomic RNA (gRNA) did not increase greatly in *N. benthamiana* when doubly infected with PVX and either Plum pox virus (PPV) or Tobacco etch virus (TEV), despite the extreme enhancement of symptoms in this host that lead to SN, i.e., synergism in pathology (González-Jara et al 2004, Pruss et al 1997). PVX-mediated expression of viral genes to determine whether a protein would function as a pathogenicity determinant is established technique (González-Jara et al 2005, González-Jara et al 2004).

Previous studies revealed that PSTVd infection induced the stress-responsive microRNA species miR398, miR398a-3p and in qRT-PCR assay, their expression levels were unusually high in hpDCL2/4i-51-72E plants (DCL2 and 4 gene knockdown) showing necrosis also the expression level of mRNAs for cytosolic Cu/Zn-superoxide dismutase 1 (i.e., SlSOD1 and SlSOD2 in tomatoes), chloroplast-localized Cu/Zn-SOD2 (i.e., SlSOD3 in tomatoes), and the copper chaperon for SOD (CCS1; i.e., SlSOD4 in tomatoes), potential targets for miRNA398, 398a-3p, and 398, respectively, declined greatly (Suzuki et al 2019). Since SODs, including CCS1 in concert with miR398 and miR398a-3p have a function in controlling the detoxification of harmful reactive oxygen species (ROS) in the cells, their regulation is very important if plants are to tolerate oxidative stresses (Beauclair et al 2010).

Recently study, systemic necrosis was correlated with when AGO2 gene suppressed in PVX infected tomato plants (Kwon et al 2020). Also, previous studies show that Similar symptom

exacerbations, including systemic necrosis, have been observed in the AGO2-knockout *N. benthamiana* using CRISPR/Cas9 (Ludman et al 2017) and Downregulation of double-stranded-RNA-Binding Protein (DRB2) by VIGS is able to reduce PVX-triggered systemic necrosis in ago2 mutant *N. benthamiana* (Fátyol et al 2020). These previous studies may help reveal the mechanism through which AGO2-knockdown alters the expression of endogenous genes and which host and viral genes involved in the development of necrotic symptoms during infection with PVX.

Based on background studies, to confirm in systemic necrotic pathoype factor challenged triggerd by PVX infection in when AGO2 gene suppressed tomato plant. And using the transient expression of viral proteins by *Agrobacterium tumefaciens* (i.e., agroinfiltration) and chimeric viruses (using two difference pathotype PVX) to demonstrated that necrotic pathotype.

MATERIAL AND METHODS

Plants and viruses

Wild-type tomato (*Solanum lycopersicum* cv. Moneymaker) and transgenic tomato (SlAGO2) plants were previously created using the host RNA silencing mechanism (Kwon et al 2020) . The binary vector pGR107, which contains the infectious cDNA of PVX, was kindly provided by D. C. Baulcombe (University of Cambridge, Cambridge, United Kingdom) and necrotic pathotype strain PVX-8 (Yatsugatake) was provided by Maoka Tetsuo (Division of Agro-Environmental Research, Hokkaido Agricultural Research Center, NARO, Japan) for the inoculation tests in this study.

Binary vector constructs

The pGR107 (PVX-Uk3 strain) expression vector (Jones *et al*., 1999) and PVX-8 used for construct chimeric viruses. The three chimeric constructs used in the study between the UK3 and -8 strains were constructed using restriction enzyme site in the PVX sequence, including *Mun*I (position 47nt), *Bln*I (position 3940nt), *Nde*I (position 5146nt) and *Xho*I (position 6380nt) in the viral cDNA infectious clones. Each of the three fragments, 3.9kb (*Mun*I-*Bln*I)/ 1.2kb (*Bln*I-*Nde*I)/ 1.2kb (*Nde*I-*Xho*I), was exchanged between the UK3 and -8 strains using these conserved restriction sites. Each chimeric vector introduced into *Agrobacterium tumefaciens* strain GV3101. PVX ORFs and *N. benthamiana* AGO2 IR (Inverted repeat) for viral gene expression and AGO2 gene suppression, were created in binary vector. *N. benthamiana* AGO2 gene (Nbv6.1trP9009 registered in the *N. benthamiana* database at https://sefapps02.qut.edu.au) repressed (NbAGO2IR) was created. The inverted repeat (IR) sequences were constructed by placing parts of AGO2 (595bp) in a head-to-head orientation across an intron sequence to create an IR sequence. The *N. benthamiana* AGO2 IR (Inverted Repeat) sequences were cloned into the *Nde*I/*Sal*I site

of the binary vector pRI201-AN (Takara) downstream of the CaMV-35S promoter and introduced into *A. tumefaciens* strain GV3101. SlSOD4 for overexpression vector was created in PVX and binary vector. *S. lycopersicum* SOD4 gene (Solyc11g066390.1 registered in the tomato genome database at https://solgenomics.net /organism/Solanum_lycopersicum/genome). The SlSOD4 complete CDS was cloned into the *Cla*I/*Sal*I site of the pGR107 vector.

Plant growth conditions and agro-mediated infiltration

Tomato and *N. benthamiana* plants were grown in a growth chamber with a 16-h light/8-h dark cycle at 25°C. For transient expression assays (leaf patch assays), *A. tumefaciens* cultures were grown to exponential phase in YEP broth with antibiotics at 28°C for 48hr. The *Agrobacterium* was then pelleted by centrifuging at 3000 rpm for 20 min, and re-suspended in agro-infiltration buffer (10 mM $MgCl_2$, 10 mM MES pH 5.7, 100 µM acetosyringone), and the concentration determined by measuring OD_{600} values. In the case of viral amplicons, bacterial cultures were diluted to a final optical density of 0.5. Equal volumes of each suspension were then combined in a 1:1 ratio.

Cell death and H_2O_2 detection

For cell death and H_2O_2 accumulation analyses, leaf discs detached from systemic leaves were stained with 3,3`-diaminobenzidine (DAB) staining to detect H_2O_2 production. leaves were vacuum infiltrated for 10 min with DAB solution at 1 mg/mL and destained using boiling into the 100% ethanol for 20 min.

Reverse transcription-polymerase chain reaction (RT-PCR) and real-time PCR

mRNA was detected using RT-PCR as follows. Tomato and *N. benthamiana* leaves were ground in liquid nitrogen, and total RNA was extracted with TRIzol™ Reagent (Thermo Fisher Scientific, Inc., Waltham, MA, USA). All RNA samples were treated with RNase-free DNase I (Roche Diagnostics, Basel, Switzerland). cDNA was synthesized from 1 μg of RNA extract using the modified Moloney Murine Leukemia Virus (MMLV) reverse transcriptase ReverTra Ace® (Toyobo, Osaka, Japan). PCR was performed to cloning chimeric PVX and endogenous mRNA. The mixture (50μl) contained cDNA corresponding to 0.1 μg RNA, 0.4 μM of each of the specific primer pairs (Supplementary Table1), 0.2 mM deoxyribonucleotide triphosphate (dNTPs), 2mM $MgSO_4$ and 0.5 U KOD Plus NEO™ DNA polymerase (Toyobo, Osaka, Japan). PCR mixtures were incubated for 2 min at 94°C, followed by 30 cycles at 94°C for 30 s, 60°C for 30 s, and 68°C for 180 s. For PR-1a were incubated for 2 min at 94°C, followed by 30 cycles of 94°C for 30 s, 60°C for 30 s, and 68°C for 30 s. Quantitative PCR (qPCR) was performed using the AriaMx real-time PCR system (Agilent Technologies, Santa Clara, CA, USA). The reaction mixture (25 μl) contained 0.3 mM (each) forward and reverse primers (Supplementary Table1), 0.2 mM dNTPs, 0.625 U Ex Taq™ DNA polymerase (Takara), SYBR Green (1/800 dilution) (Thermo Fisher Scientific), and cDNA obtained by reverse transcribing 50 ng of total RNA. Samples were incubated for 2 min at 95°C, followed by 39 cycles at 95°C for 10 s, and at 58°C and 72°C for 20 s each.

Northern and western blotting assays

Accumulation of the PVX CP, genomic RNA and PR-1a (pathogenesis-related protein 1a) gene were investigated through western and northern blotting as previously described (Jeon et al 2017). Upper uninoculated leaves from each plant at 10, 15 and 20 days post-inoculation (dpi) were harvested and total RNA preparations (1–10 μg) were extracted using the TRIzol™ Reagent. After

denaturing the RNA extracts by heating at 65℃ for 15 min in a solution containing RNA denaturation buffer (0.9 M disodium phosphate, 0.1 M monosodium phosphate, 37% formaldehyde, 0.05% formamide), the samples were loaded into 1.4% agarose gels containing 5% formaldehyde and 1×3-(N-morpholino) propanesulfonic acid buffer and run at 100 V for 30 min. Following transfer to a nylon membrane (Hybond-N; GE Healthcare, Chicago, IL, USA), hybridization with a digoxigenin-labeled probe (Roche Diagnostics) was performed to detect the 3′ -terminal regions of PVX genome segments. Chemiluminescence signals with CDP-star (Millipore Sigma, St. Louis, MO, USA) were quantitatively detected using a LAS-4000 mini-imaging system (GE Healthcare). sRNA and miRNA also performed by northern blot assay. Total RNAs (~10 μg) extracted from each sample were separated in 12% PAGE containing 8M urea and 0.5X tris boric acid edta (TBE) buffer and run at 200V for 2hr. transferred to nylon membrane on semidry method in 10V for 1hr, and analyzed by RNA gel-blot hybridization analysis using a DIG-PVX-cRNA or miR398a-3p probe (Suzuki et al 2019).

Western blotting was conducted as previously described (Nakahara et al 2012). Total proteins were separated through electrophoresis in 12% sodium dodecyl sulfate-polyacrylamide gel electrophoresis Bis-Tris gels using Tris-glycine buffer, followed by electro-transfer onto a polyvinylidene difluoride membrane. For detection of viral coat protein and SlSOD proteins, primary antibodies raised against PVX CP provided by Japan Plant Protection Association and Flag-tag monoclonal antibody (Wako, Japan), were used at a 1:1000 dilution, while alkaline phosphatase-conjugated goat antirabbit (Thermo Fisher Scientific) or antimouse immunoglobulin G (Biorad, USA) was used as the secondary antibody. Chemiluminescence signals were detected using the CDP-Star reagent in a LAS-4000 mini-imaging system.

RESULTS

AGO2 gene suppression enhances systemic necrosis with PVX infection

The hpAGO2.3 transgenic tomato plants and *N. benthamiana* inoculated with PVX observed symptoms in the non-inoculated upper leaves of all inoculated plants at 6 dpi (Figure 2-1). The symptoms that developed in hpAGO2.3 were more severe than those that developed in the inoculation plants. Specifically, necrotic spots began to develop in hpAGO2.3 plants on the second upper leaf from the inoculated leaf at 3 dpi, and the necrotic symptoms spread systemically at 15 dpi. Meanwhile, the systemic necrotic symptoms that developed in PVX-8 infected *N. benthamiana* but PVX-UK3 only developed systemic mosaic symptom (Figure 2-1). The 3,3`-diaminobenzidine (DAB) staining detected the accumulation of H_2O_2 (Figure 2-1). The accumulation of genomic RNA was analyzed by northern blotting (Fig 2-1) to determine whether the difference in symptoms was associated with the multiplication of PVX in these plants. In PVX-UK3 infection, PVX viral RNA accumulation significantly was higher than wild type tomato plants in 10 dpi to 20dpi (Figure 2-1). This result show that, necrosis symptoms induced in hpAGO2.3 by PVX infection is not related to viral accumulation. In addition, northern blot show that necrosis pathotype in PVX-8 infected in hpAGO2.3 and wild type plants and that the viral accumulation in hpAGO2.3 was higher than that of wild type (Figure 2-2). In the non-inoculated symptomatic leaves of PVX infected hpAGO2.3, northern blot analysis revealed robust induction of PR-1a (markers for virus induced SN), while their levels did not change significantly in the wild type plants (Figure 2-2). Also, virus derived small interfering RNAs (vsiRNAs) accumulation (21nt-24nt) was significant different between hpAGO2.3 and WT (Figure 2-2). These results confirmed that PVX infection elicited a strong necrotic response in the ago2 plants.

In order to identify the region of the genome responsible for the differences in the symptoms caused by PVX-UK3 and PVX-8, various chimeric cDNA clones were constructed. The

restriction enzyme sites used to produce the chimeras were a *Mun*I site (nt 47) located within the 5′-untranslated regions of the genome, a *Bln*I site (nt 3940) located close to the 3′-end of ORF1, an *Nde*I site (nt 5146) located close to the 3′-end of TGB1, which includes the start codon of TGB2, and an *Xho*I (nt 6380) site located downstream from the poly(A) sequence in the plasmid vector sequence (Figure 2-3). *N. benthamiana* were infiltrated with each of the chimera cDNA clones. At 3 days-post-infiltration (dpi), the PVX-UNU chimera induced necrosis both single infiltration and NbAGO2IR co-infiltration (Figure 2-3). In contrast, pGR107 (UK3 strain) and PVX chimeras (NUU and UUN) induced necrosis only NbAGO2IR co-infiltration also DAB staining results show that H_2O_2 accumulation was detected in the necrosis (Figure 2-3). On RT-qPCR result showed that *N. benthamiana* AGO2 gene down-regulated by inverted repeat (Figure 2-3). In the western blot, the PVX coat protein accumulation was not significant different in between pGR107 and PVX chimeras.

(A)

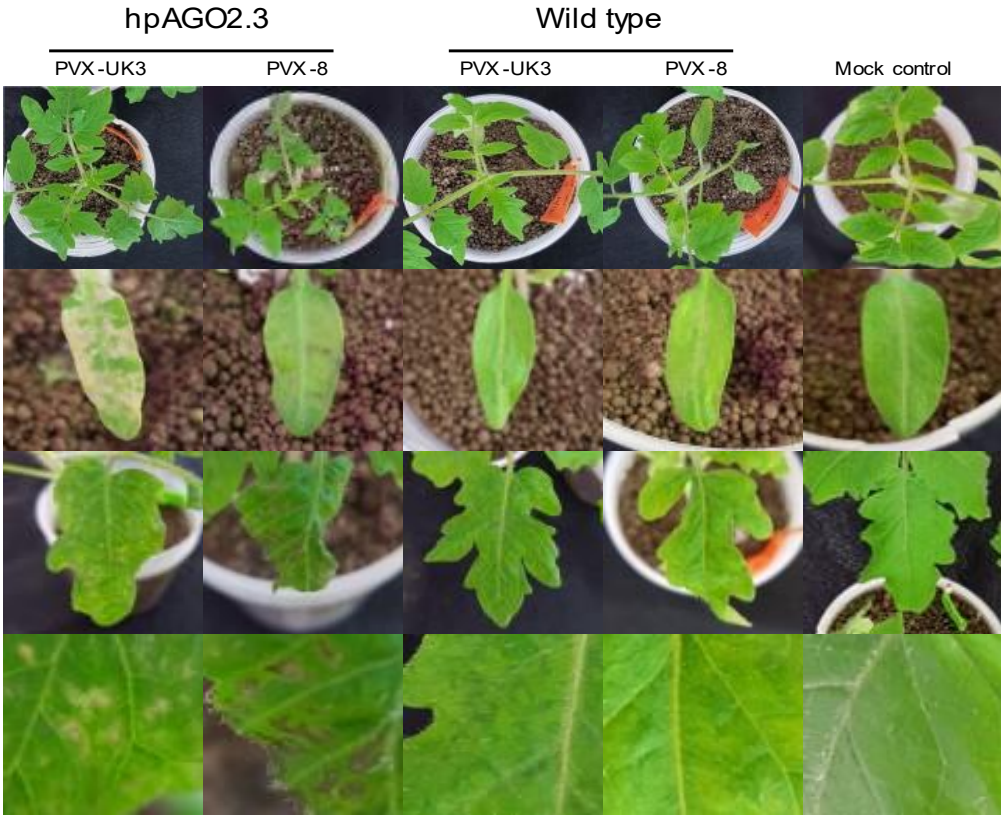
hpAGO2.3
Wild type
PVX-UK3
PVX-8
PVX-UK3
PVX-8
Mock control

(B)

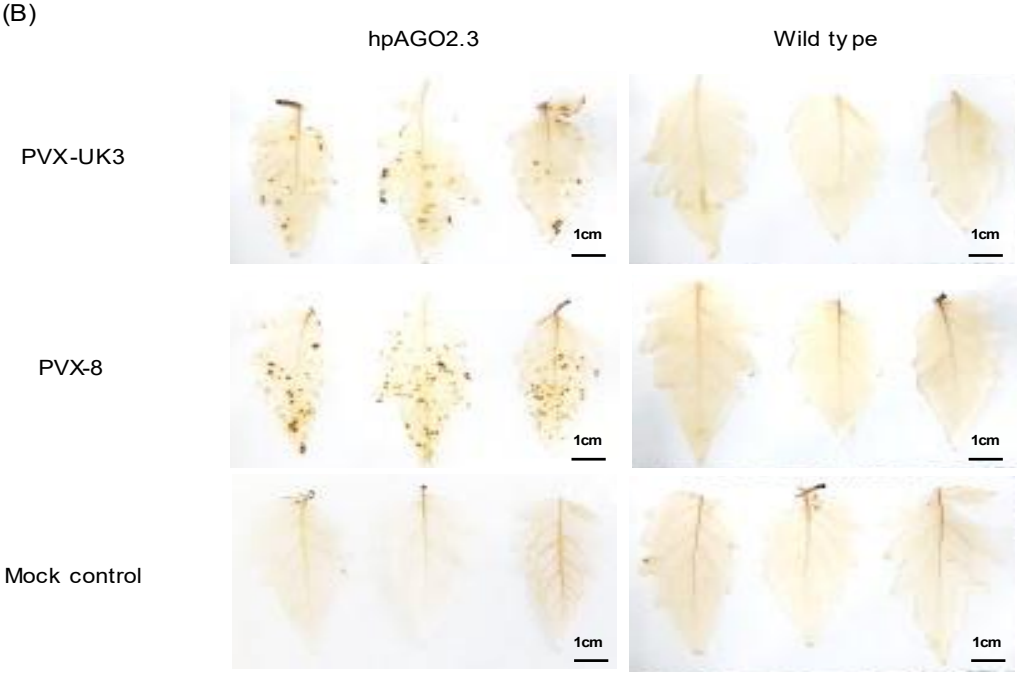
hpAGO2.3
Wild type
PVX-UK3
PVX-8
Mock control
1cm
1cm
1cm
1cm
1cm
1cm

Fig 2-1 Reactions of transgenic plants following mechanical inoculation with PVX-UK3 and PVX-8. (A) Symptoms developed in AGO2-knockdown tomato plants (hpAGO2) inoculated with PVX-UK3 and PVX-8. Photographs were captured at 10 days-post-inoculation (dpi). Moneymaker tomato plants were also inoculated with PVX (wild type) and buffer (Mock) as controls. (B) Upper leaves were stained with DAB solution at 10 dpi. DAB formed a deep brown polymerization product upon reaction with H^2O^2.

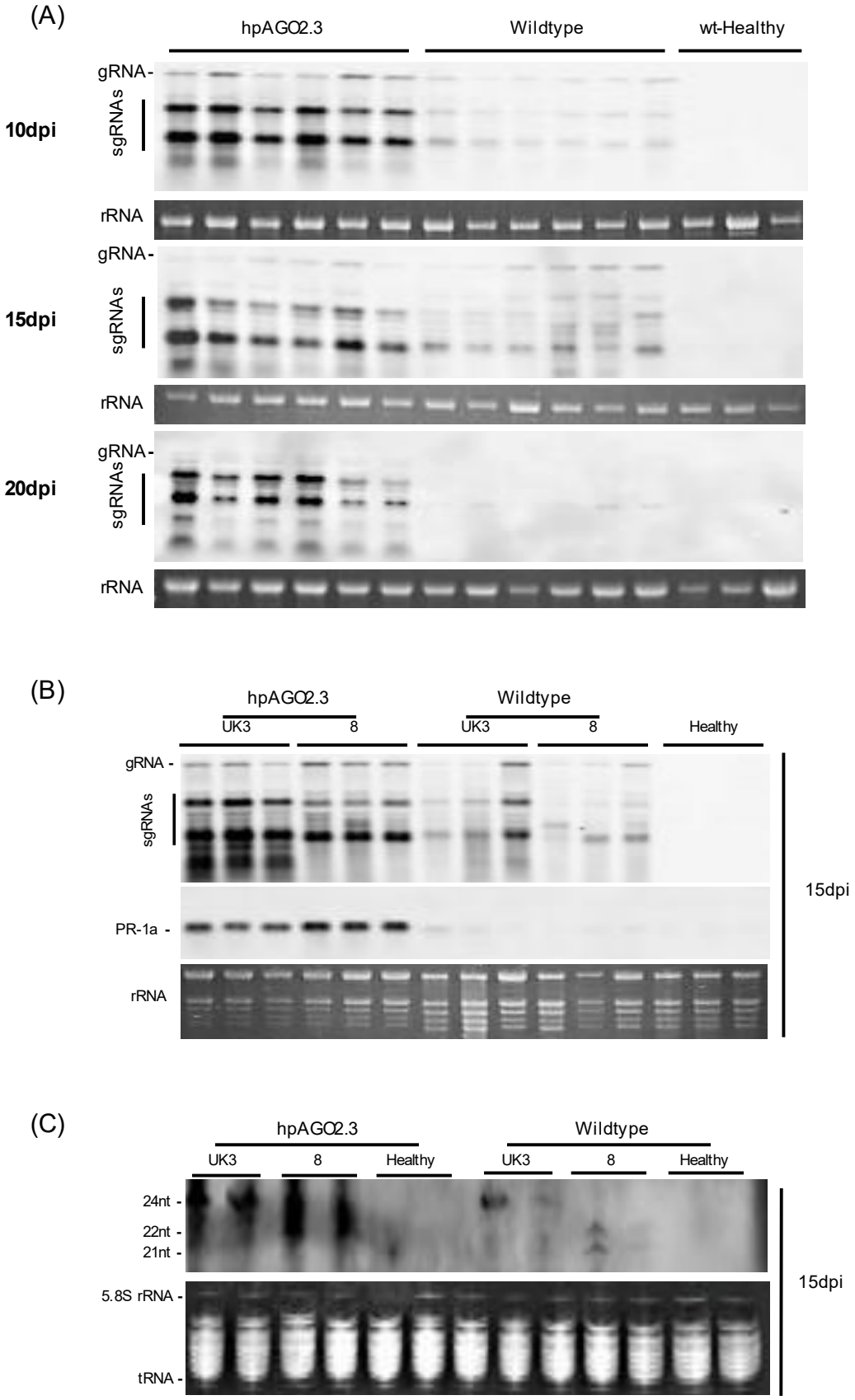
(A)
hpAGO2.3
Wildtype
wt-Healthy
10dpi
gRNA
sgRNAs
rRNA
15dpi
gRNA
sgRNAs
rRNA
20dpi
gRNA
sgRNAs
rRNA
(B)
hpAGO2.3
Wildtype
UK3
8
UK3
8
Healthy
gRNA
sgRNAs
PR-1a
rRNA
15dpi
(C)
hpAGO2.3
Wildtype
UK3
8
Healthy
UK3
8
Healthy
24nt
22nt
21nt
5.8S rRNA
tRNA
15dpi

Fig. 2-2 Northern blot analysis of total RNA extracted from upper leaves at 15 dpi. (A) Total RNAs (~10 μg) extracted from transgenic lines (hpAGO2) and wild type tomato plants inoculated with PVX-UK3 and PVX-8 were separated in 8M-urea 12% PAGE, transferred to nylon membrane, and analyzed by RNA gel-blot hybridization analysis using a DIG-PVX-cRNA probe. tRNA and 5s RNA shows the loading control stained with ethidium bromide (EtBr). (B) Total RNAs extracted from transgenic lines (hpAGO2) and wild type tomato plants inoculated with PVX-UK3 and PVX-8 at 15 dpi were fractionated using an agarose gel to detect the PVX genomic (gRNA), subgenomic RNAs (sgRNAs) and pathogenesis related 1a gene (PR-1a) in non-inoculated upper leaves. rRNA was used as loading control. (C) Northern-blot hybridization of vsiRNA (viral derived small interfering RNA). Aliquots (10 μg) of total RNA, isolated at 15dpi, were fractionated by electrophoresis in 8M-urea 12% PAGE, transferred to nylon membrane, and hybridized with a DIG-labeled cRNA probe for DIG-PVX-cRNA probe. tRNA and 5s RNA shows the loading control stained with ethidium bromide (EtBr).

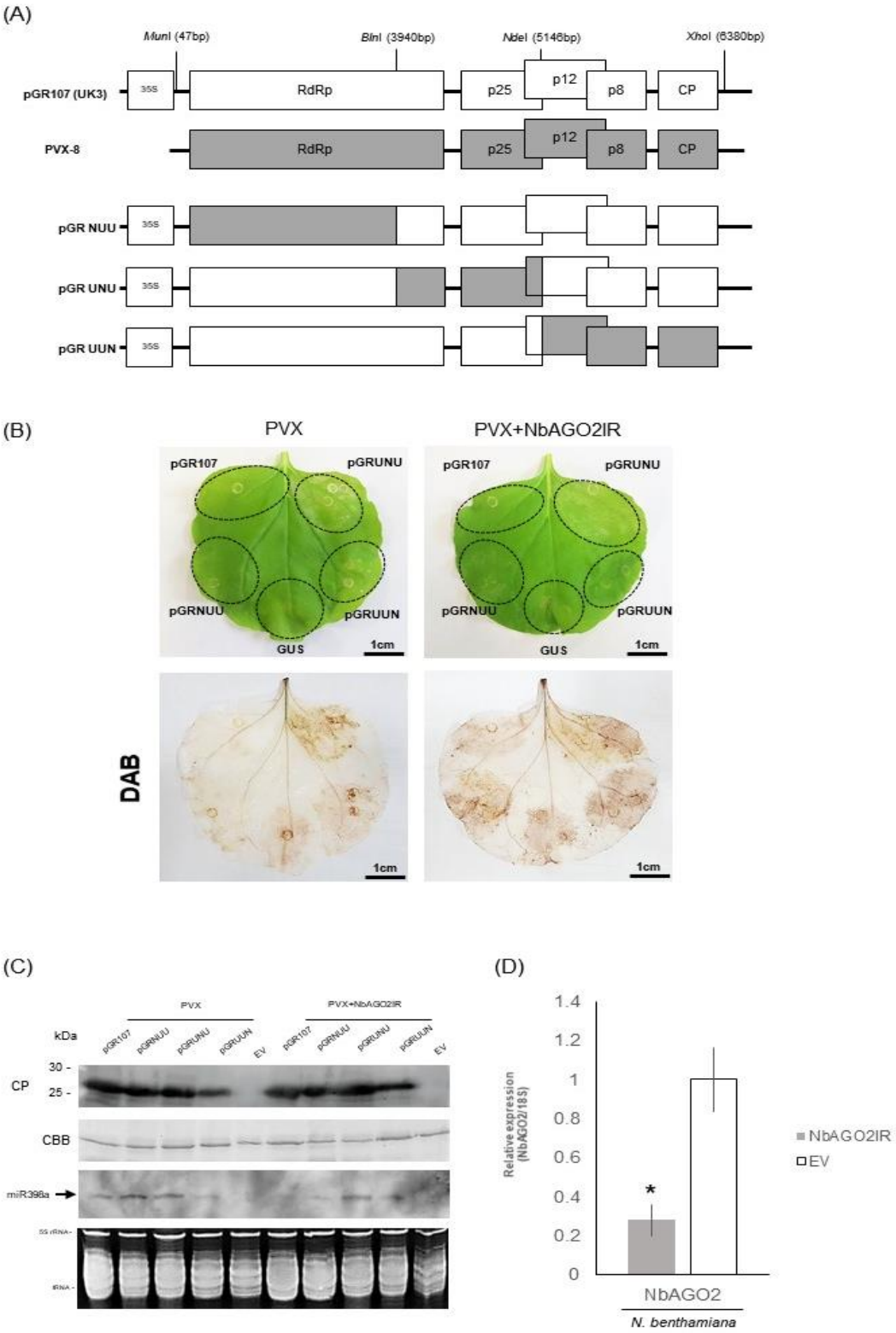
(A)
MunI (47bp)
BlnI (3940bp)
NdeI (5146bp)
XhoI (6380bp)
pGR107 (UK3)
35S
RdRp
p25
p12
p8
CP
PVX-8
pGR NUU
pGR UNU
pGR UUN
(B)
PVX
PVX+NbAGO2IR
pGR107
pGRUNU
pGRNUU
pGRUUN
GUS
1cm
DAB
(C)
PVX
PVX+NbAGO2IR
kDa
pGR107
pGRNUU
pGRUNU
pGRUUN
EV
30 -
25 -
CP
CBB
miR398a
5S rRNA
tRNA
(D)
Relative expression (NbAGO2/18S)
1.4
1.2
1
0.8
0.6
0.4
0.2
0
*
NbAGO2
N. benthamiana
NbAGO2IR
EV

Fig. 2-3. Expression of PVX together with chimera virus elicits an necrosis in *N. benthamiana.* (A) Schematic representation of the PVX genome of PVX-8, pGR107 infectious clone, and derivative constructions. The ORFs of sequences derived from pGR107 and PVX-8 are shown as light and dark boxes, respectively. Constructs made using restriction enzymes and recombinant PCR are shown in PVX genome. (B) Leaves of *N. benthamiana* were infiltrated with *Agrobacterium* cultures containing binary constructs expressing pGR107(UK3 strain) and PVX chimera viruses. Photographs were captured at 7 dpi (upper panel). Upper leaves was stained with DAB solution at 15 dpi (down panel). (C) Total protein samples were prepared from infiltrated leaf disc pGR107 and PVX chimera viruses at 7 dpi. Samples were also prepared from the empty vector infiltrated leaf disc (EV) as controls. The CBB-stained gel was used as a loading control (RUBISCO protein). (D) Relative expression levels of AGO2 on infiltrated leaves in *N. benthamiana*. Total RNA was extracted at 6 day-post-infiltration (dpi). The relative expression levels of mRNAs were estimated by real-time reverse transcription-polymerase chain reaction (RT-PCR). Using 18s ribosome RNA as a housekeeping gene. Error bars represent standard errors. Student's t-test was applied to analyze the data, comparing dsRNA-expressing and empty vector infiltrated on leaf tissue. Each analysis consisted of three biological replicates collected three plants per treatment. The values with the single asterisk (*; $p < 0.05$) were statistically significant at and 5% levels compared to EV-infiltrated tissue.

SOD4 controlled systemic necrotic in hpAGO2 transgenic tomato plants when PVX-infection

In previous study, miR398a-3p is a miRNA that negatively regulates superoxide dismutase **(**SOD), which normally scavenges harmful ROS. When *A. thaliana* is exposed to oxidative stress arising from biotic or abiotic factors, the miR398a-3p expression was down-regulated at the level of transcription, and as a result, the post-transcriptional accumulation of Cu/Zn-SOD1 and Cu/Zn-SOD2 mRNAs is up-regulated, leading to scavenging ROS (Sunkar et al 2006). Based on the previous studies, The expression level of miRNA398a-3p was analyzed during PVX infection. In northern blot assay, miR398a-3p was not detectable in healthy plants from either line, indicating that the expression levels of miR398a-3p were very low. In contrast, in PVX-infected plants, miR398a-3p reached detectable levels at 15dpi (Fig 2-4), indicating that PVX infection stimulates the expression of miR398a-3p. The target sequence of miR398 was confirmed in the gene sequence of SlSOD1 and SlSOD2, and the target sequence of miR398a-3p was confirmed in the gene sequence of SlSOD3. In addition, SlSOD4, which is reported to have Cu/Zn and heavy-metal binding motifs (Feng et al 2016) has a nucleotide sequence similar to the CCS1 sequence reported previously (accession number NM_001347085, AK319564) and has the target sequence of miR398. Based on these findings, correlations among the expression level of SlSOD1, SlSOD2, SlSOD3 and SlSOD4 were analyzed using RT-qPCR. Three plants each from lines hpAGO2.3 and wild type were infected with PVX. Each leaf different position was harvested at 15dpi for RNA extraction, when symptoms of systemic necrotic started to develop in upper leaves. The result show that SlSOD3 was down regulated both the PVX-UK3 and PVX-8 in hpAGO2.3 and wild type tomato plants and the expression level of SlSOD4 was down-regulated almost 50% in hpAGO2.3 inoculated with PVX-UK3 and PVX-8 (Figure 2-4). In contrast, the SlSOD1 expression was not significantly different in both hpAGO2.3 and wild type (Figure 2-4). In notably, SlSOD2 gene up-regulated almost 177 to 642% under PVXs infection in wild type tomato plants (Figure 2-4). It is necessary to further analyze the expression levels of miR398 in

these leaves to clarify whether the high level of miR398 expression and down-regulation of SlSOD4 mRNAs are also involved in the onset of necrosis symptoms observed in hpAGO2.3.

Therefore, we cloned the SOD4 complete protein coding sequence (CDS) into both pGR107 and pGRUNU (Necrotic pathotype) PVXs, followed by inoculation and co-expression in hpAGO2.3 (Figure 2-5). At 15dpi, systemic necrotic symptom was significantly different between the PVX and SOD4 co-expression in hpAGO2.3 transgenic plants (Figure 2-5). In a western blot assay, PVX-CP and Flag-tagged SOD4 protein were observed at 15dpi (Figure 2-5). Also, severe systemic necrotic was induced in the pGRUNU infiltration but in contrast, pGRUNU and SOD4 co-expressed PVX construct was inhibited systemic necrotic in hpAGO2.3 (Fig 2-5). To confirm it systemic necrosis was inhibited by co-expression of SOD4 cloned SOD4 site-direct stop codon mutant (Figure 2-6) into pGRUNU PVX, and conducted inoculation and co-expression. As expected, co-experssion of PVX-SOD4 and PVX-SOD4 mutant significant different symptoms in. hpAGO2.3 transgenic line (Figure 2-6). In a western blot results, the SOD4 protein was observed in the pGRUNU co-expression but not the SOD4 mutant (Figure 2-6).

Based on the above results, systemic necrotic symptom induced by PVX infection when suppressed by SOD4 and, necrotic symptom controlled by tomato (hpAGO2.3 transgenic) in which AGO2 expression was suppressed.

(A)

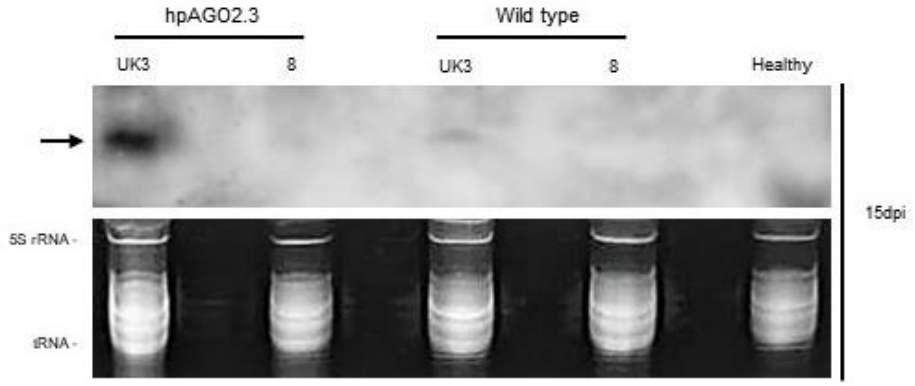
hpAGO2.3
Wild type
UK3
8
UK3
8
Healthy
5S rRNA
tRNA
15dpi

(B)

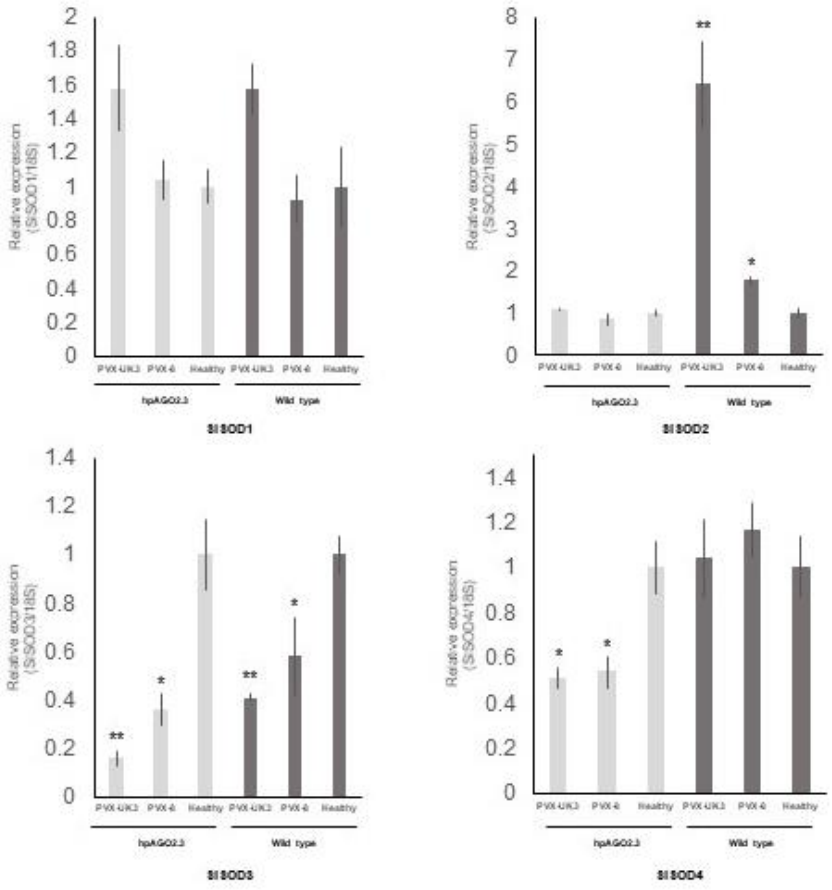
Relative expression (SlSOD1/18S)
Relative expression (SlSOD2/18S)
Relative expression (SlSOD3/18S)
Relative expression (SlSOD4/18S)
PVX-UK3
PVX-8
Healthy
hpAGO2.3
Wild type
SlSOD1
SlSOD2
SlSOD3
SlSOD4

Fig 2-4 Analysis of miR398a-3p, tomato SODs expression levels in healthy leaves and PVX-infected leaves with or without showing necrosis. (A) Northern-blot hybridization of miR398a-3p. Aliquots (10 μg) of total RNA, isolated at 15dpi, were fractionated by electrophoresis in 8M-urea 12% PAGE, transferred to nylon membrane, and hybridized with a DIG-labeled cRNA probe for miR398a-3p. tRNA and 5s RNA shows the loading control stained with ethidium bromide (EtBr). (B) Relative expression levels of the SOD1, SOD2, SOD3 and SOD4 mRNAs in transgenic lines (hpAGO2.3) and wild type tomato plants expressing dsRNAs, compared with healthy controls. The relative levels of these mRNAs were investigated through real-time reverse transcription-polymerase chain reaction (RT-PCR) using the 18s ribosome RNA as control. Student's t-test was applied to analyze the data, comparing dsRNA-expressing and wild type tomato plants. Asterisks indicate a statistically significant difference in mRNA accumulation of the gene between plants with/without expressing dsRNA ($P<0.05$).

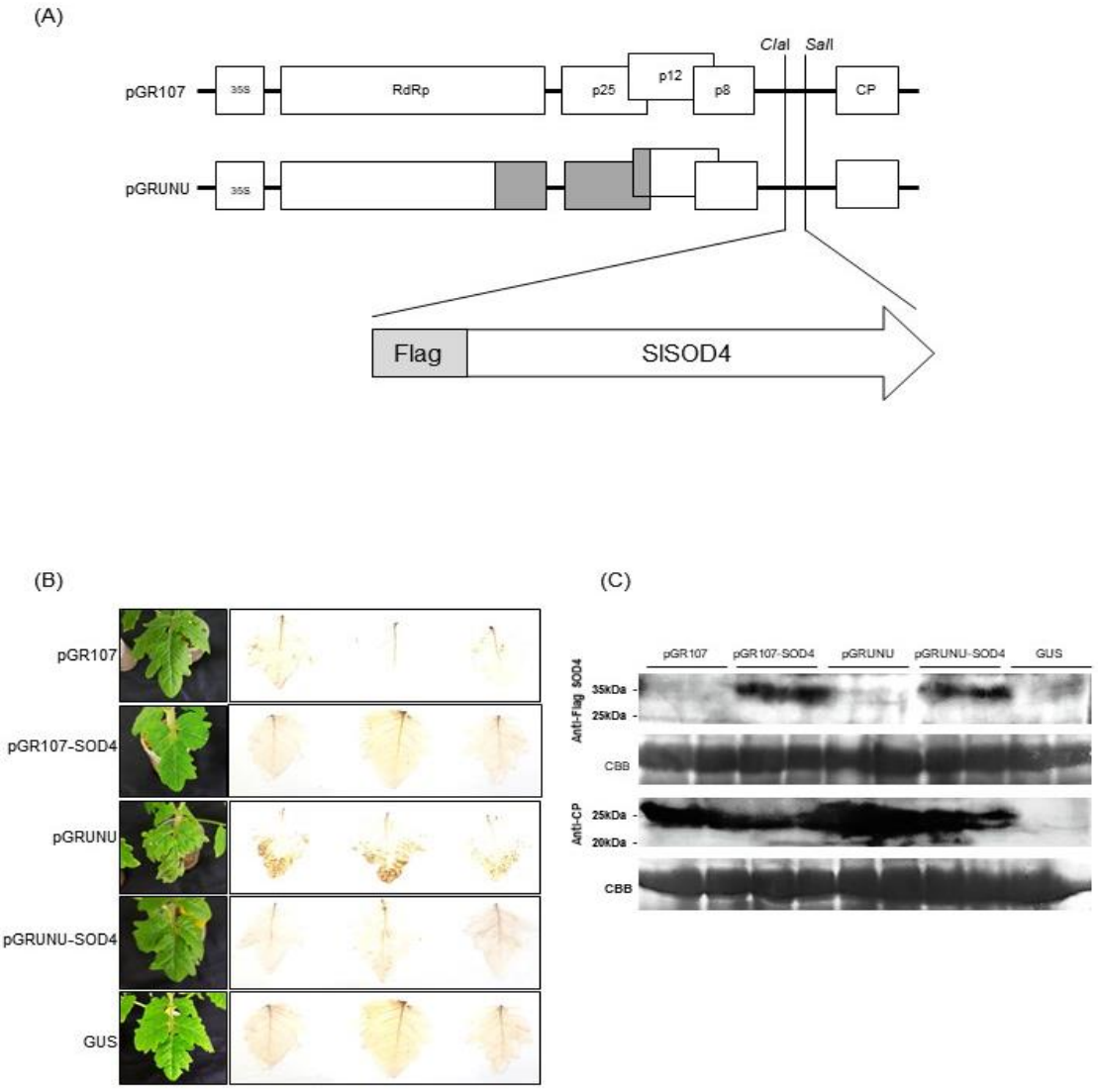

Fig 2-5 Expression of PVX together with SOD4 and suppressed an necrosis in hpAGO2.3

(A) Schematic representation of the PVX genome of PVX-8, pGR107 infectious clone, and derivative constructs The ORFs of sequences derived from pGR107 and PVX-8 are shown as light and dark boxes, respectively. SlSOD4 complete cds was cloned into the *Cla*I and *Sal*I. (B) Symptoms developed in AGO2-knockdown tomato plants (hpAGO2.3) inoculated with PVXs. Photographs were captured at 10 days-post-infiltration (dpi). Moneymaker tomato plants were also infiltrated with β-Glucuronidase (GUS) gene as controls. Upper leaves were stained with DAB solution at 10 dpi. DAB formed a deep brown polymerization product upon reaction with H^2O^2. (C) For the detection of SOD4 and CP, total protein was extracted from the upper leaves

of tomato plants (hpAGO2.3) infiltrated with PVXs and β-Glucuronidase (GUS) gene at 10 dpi. The CBB-stained gel was used as a loading control.

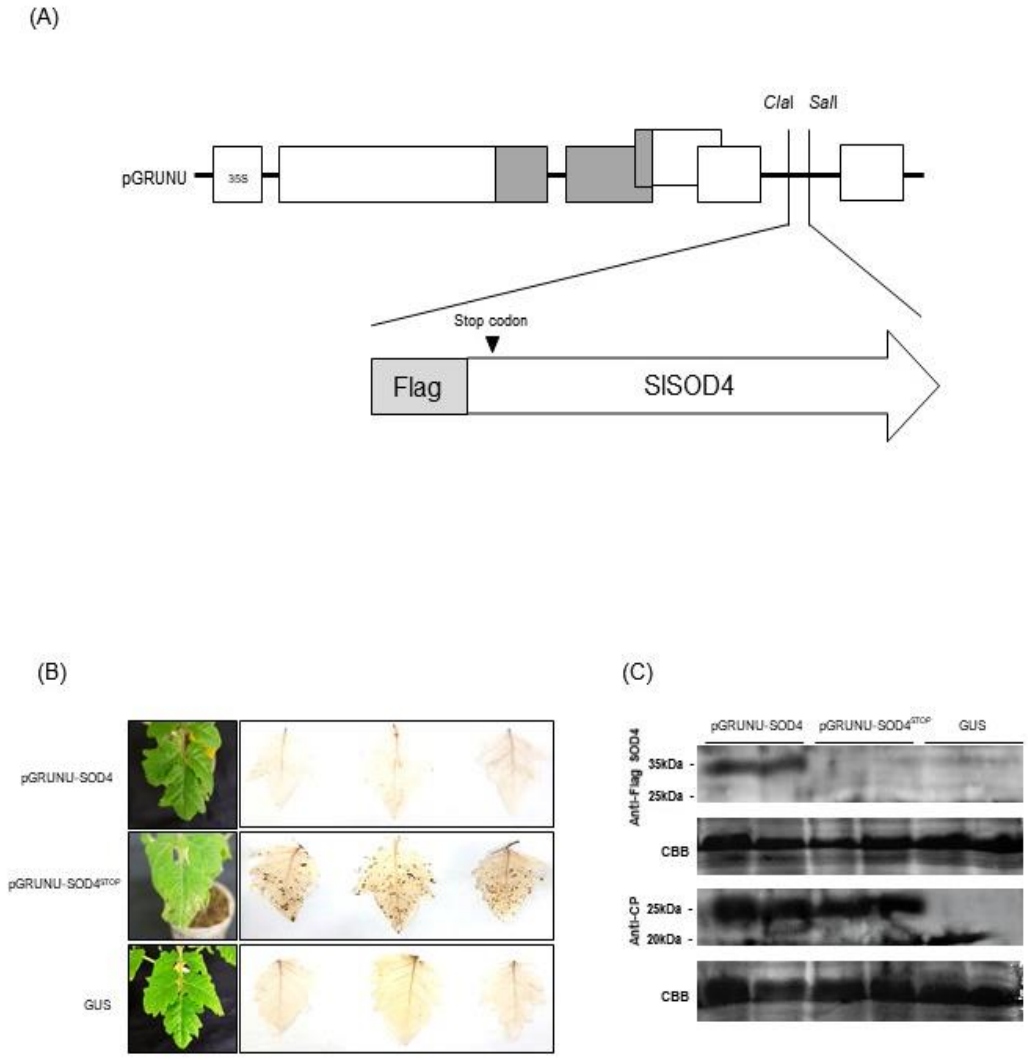

Fig 2-6 Expression of PVX together with SOD4 mutant and induced an necrosis in hpAGO2.3 (A) Schematic representation of the PVX genome of pGRUNU infectious clone, and derivative constructions. The ORFs of sequences derived from pGR107 and PVX-8 are shown as light and dark boxes, respectively. SlSOD4 complete cds was cloned into the *Cla*I and *Sal*I. (B) Symptoms developed in AGO2-knockdown tomato plants (hpAGO2.3) infiltrated with PVXs. Photographs were captured at 10 days-post-infiltration (dpi). Moneymaker tomato plants were also infiltrated with β-Glucuronidase (GUS) gene as controls. Upper leaves were stained with DAB solution at 10 dpi. DAB formed a deep brown polymerization product upon reaction with H^2O^2. (C) For the detection of SOD4 and CP, total protein was extracted from the upper leaves

of tomato plants (hpAGO2.3) infiltrated with PVXs and β-Glucuronidase (GUS) gene at 10 dpi. The CBB-stained gel was used as a loading control.

DISCUSSION

Using the RNAi-mediated method, AGO2 knockdown 'Moneymaker' tomato lines were produced and transformed with an IR construct consisting of partial sequences of tomato homologs SlAGO2a, SlAGO2b and SlAGO3 and transgenic lines, hpAGO2.3, was shown systemic necrotic symptoms upon PVX infection (Kwon et al 2020). This phenomenon has also been reported in previous studies that, systemic necrosis, has been observed in the AGO2-knockout *N. benthamiana* using CRISPR/Cas9 (Ludman et al 2017) and the downregulation of double-stranded-RNA-Binding Protein (DRB2) by VIGS is able to reduce PVX-triggered systemic necrosis in ago2 mutant *N. benthamiana* (Fátyol et al 2020). However, systemic necrosis induced from PVX infection by the expression level of AGO2 was not clearly identified.

The previous study shows that miR398 and miR398a-3p are stress-responsive miRNAs, known to be expressed in response to various stresses, that inhibit the expression of cytosolic- and chloroplast-localized SODs (Juszczak and Baier 2012) and copper chaperons for SOD (i.e., CCS1) (Beauclair et al 2010), which scavenge harmful ROS. Northern-blot hybridization analysis clearly showed that miR398a-3p was detected exclusively from the PVX-infected plants (both UK3 and PVX-8), with the intensity of the bands approximately higher in PVX-hpAGO2.3 compared with PVX-WT. These results, along with the observation that PVX-hpAGO2.3 experienced severe systemic necrosis, strongly suggested that ROS are generated in PVX-hpAGO2.3. The highest ROS production and scavenging activities were found in leaves showing necrosis in line PVX-hpAGO2.3, indicating that ROS were actively generated and then rapidly scavenging in the plants. In contrast, even after PVX infection, wild type did not show any visible necrotic symptoms or excessive ROS production.

Some miRNAs appear to repress gene expression through both translational inhibition and target cleavage. This raises a question of how translation inhibition vs. target cleavage is determined. A recent study shows that miRNAs display stronger translational inhibition in a transient assay when

their binding sites are localized in the 50 coding region (Li JF et al 2013), while another study reveals that miRNAs enhance translational repression in male germ cells of plants (Grant-Downton et al 2013). These results suggest that multiple factors help cells to select translational repression or target cleavage. In some cell types, the concurrence of translational inhibition and cleavage happens. A considerable amount of AGO1 is associated with the endoplasmic reticulum (ER) (Li et al 2013). In addition, lack of altered meristem program1 (AMP1), an integral ER membrane protein, impairs miRNA-mediated translational repression, but not target transcript cleavage, suggesting that ER may be a site for translational inhibition to occur (Li et al 2013). Agreeing with this notion, amp1 reduces the exclusion efficiency of target mRNAs from membrane bound polysomes (Li et al 2013). The unusually higher levels of ROS production in PVX-hpAGO2.3 seems to be a major reason for the development of severe necrotic reactions in these plants. More specifically, miR398 and 398a-3p must be down-regulated under the normal conditions in order to enhance the function of SODs when ROS are produced following a virus infection.

Also, the production of ROS is an important defence reaction against pathogens which is rapidly induced upon recognition of a pathogen attack. Recent data from comprehensive and global transcriptome and metabolome analyses suggested that viroid infections trigger plant immune responses and result in the activation of various signal pathways and associated activities, such as MAPK3, PR1,1,3-beta-glucanase, and ROS biogenesis (Zheng et al 2017, Xia et al 2017). On the other hand, ROS are harmful substances that can cause significant damage to cell structures. Therefore, the proper management of ROS production and scavenging is very important when plants are protecting themselves against pathogen attacks. The results presented in this study identified several factors (i.e., miR398, miR398a-3p, Cu/Zn-SOD4, CCS1, and ROS) in tomato plants which are responsible for causing necrosis, one of the most typical and serious disease symptoms induced by PVX infections, and revealed the existence of an unresolved relationship

between AGO2 and AGO3, key of factor in RNA silencing against PVX, and the cell mechanism used to control ROS biogenesis.

Chapter 3

Genome-editing of the dicer-like 3 gene unexpectedly confers antiviral resistance in tomato

INTRODUCTION

The discovery of nucleic acid guided nucleases (NGNs) has fundamentally influenced molecular biology in the last two decades. Directing nucleases to their substrates using the simple rules of Watson-Crick base pairing serves the basis for a number of gene regulatory and defensive mechanisms employed by both prokaryotes and eukaryotes. In eukaryotes, one of the best-studied NGN-based processes is RNA silencing (or RNA interference, RNAi), which is also a major antiviral defense mechanism in plants (Wilson and Doudna et al 2013, Voinnet 2009, Martinez et al 2013, Ding 2010, Carthew and Sontheimer 2009, Baulcombe 2004, Csorba et al 2015). RNA silencing plays key roles in regulating endogenous gene expression, suppressing transposon activity, silencing transgenes, responding to environmental stimuli and combatting viral infection (Achkar et al 2016, Li et al 2017). Small RNAs (sRNAs), including miRNA and siRNA, are loaded into an Argonaute (AGO) effector protein to form RNA-induced silencing complexes to repress complementary target RNA at a posttranscriptional gene silencing (PTGS) level through cleavage and/or the inhibition of translation. RISC can also repress gene expression at a transcriptional gene (TGS) silencing level (Holoch et al 2015, Blevins et al, 2015). sRNAs are generated by DCL proteins. In *Arabidopsis*, four DCL family proteins have been found to cleave stem-loop or double-stranded (ds) RNA precursors into miRNAs or siRNAs of specific sizes (Fukudome and Fukuhara 2017). DCL1 primarily processes hairpin RNA into the 21-nt miRNA that is involved in PTGS (Zhu et al 2013, Kravchik et al 2014). However, DCL1 can also produce 22-nt miRNAs from bulged precursors that in turn lead to the production of secondary siRNAs. DCL2 is required for the biogenesis of 22-nt siRNAs from endogenous inverted repeat loci (Wu et al 2017). DCL3 produces TGS-engaged 24-nt siRNAs from RNA-dependent RNA Polymerase 2 (RDR2)-dependent dsRNAs (Blevins et al 2015, Kravchiket al 2014). DCL4 produces 21-nt siRNAs from RDR6-dependent dsRNA in the PTGS pathway (Yifhar et al 2012, Song et al 2012). NGN-based mechanisms are also employed by prokaryotes to protect the integrity of their genome (Jinek et al 2012, Doudna and Charpentier 2014, Hochstrasser and Doudna, 2015).

Adaptive immune systems, based on the concerted actions of clustered regularly interspaced short palindromic repeat (CRISPR) loci and CRISPR associated (Cas) endonucleases, help the elimination of invading genetic parasites such as viruses and plasmids in many species of archaea and eubacteria. At the end of 2012, a breakthrough paper reported a repurposed version of the type II CRISPR system from *Streptococcus pyogenes* (Jinek et al 2012). In the modified system, the Cas9 endonuclease is programmed with an engineered single guide RNA (sgRNA), allowing the cleavage of any 20nt DNA sequence that lies 5′ to an NGG motif (PAM, protospacer adjacent motif). Soon after, it was shown that the SpCas9 protein could find and cleave its target sequence not only in bacteria but in the chromatin context of higher eukaryotes as well (Cong et al 2013, Mali et al 2013). The introduced double strand DNA break can be repaired either by homologous recombination (HR), if appropriate template is present, or more frequently by the error-prone non-homologous end-joining (NHEJ) pathway. Since then, due to its simplicity and robustness, the system has been successfully adapted to gene inactivation and genome editing in many organisms, including a number of plant and animal species (Harrison et al 2014, Barrangou and Doudna 2016, Wang et al 2016).

The genome of the *S. lycopersicum* encodes 7 DCL proteins, of which the antiviral roles of DCL1, DCL2a, DCL2b, DCL2c, DCL2d, DCL3 and DCL4 have been demonstrated (Bai et al 2012).

An analysis of tomato DCL1 and DCL3-silencing mutants indicates that DCL1 produces canonical miRNAs and a few 21-nt siRNAs (Kravchik et al 2014) and DCL3 is involved in the biosynthesis of heterochromatic 24-nt siRNAs and long miRNAs (Kravchik et al 2014). DCL4 is required for the production of 21-nt tasiRNAs that in turn target the ADP-ribosylation factors (ARFs) to alter tomato leaf development (Yifhar et al 2012). Extended number of the DCL2 genes, i.e., DCL2a, DCL2b, DCL2c, and DCL2d, are encoded in tomato (Bai et al 2012). Recently, the DCL2b-dependent miRNA pathway in tomato affects the susceptibility to PVX and TMV (Wang et al 2018) also DCL2b is also required for the biosynthesis of 22-nt small RNAs to defense against ToMV (Wang et al 2018).

DCL proteins play central roles in antiviral and antibacterial responses (Bouche et al 2006, Navarro et al 2006, Ruiz-Ferrer and Voinnet 2009). They dice the dsRNA precursors of smRNAs that are critical to plants' ability to respond to the abiotic and biotic stresses that orchestrate changes in corresponding transcripts involved in resistance (Phillips et al 2007, Pandey et al 2008, Ruiz-Ferrer and Voinnet 2009). Until now, its widespread use as a model organism has been greatly hampered by the fact that like many members of the *Solanum* genus, *S. lycopersicum* has an amphidiploid genome. This feature significantly hiders the generation of genetic mutants of this plant. Importantly, the advent of the CRISPR/Cas9 technology can offer a solution for the above problem by allowing efficient production of mutants of this genetically intractable species. To avoid these problems, dcl3 mutants of *S. lycopersicum* were generated, using the CRISPR/Cas9 system. The created mutant plants were challenged with a number of viruses. The susceptibility of the dcl3 plants to different viruses varied significantly. For the first time, conclusive proof was provided for the involvement of dcl3 in antiviral immunity in a plant species other than *A. thaliana*.

MATERIAL AND METHODS

Materials and methods

Binary plasmid construction

This study used two vectors, pUC19-AtU6oligo and pZK_gYSA_FFCas9 (Mikami et al 2015, Kanazashi et al 2018), to create the binary vector pZK_AtU6gRNA_FFCas9_NPTII, following the method described by Osmani et al. (2019). Guide RNA (gRNA) recognition sites in tomato were found using CRISPRdirect (https://crispr.dbcls.jp/). The sense and antisense oligonucleotide sequences (5'-CCGAGGTGGCTCTGATGTGC-3' and 5'- GCACATCAGAGCCACCTCGG-3', respectively), including the nucleotide sequence of a target site in the Dicer-like 3 gene on chromosome 8 were synthesized and annealed to a pair of oligonucleotides for the gRNA to DCL3. The annealed oligonucleotides were cloned into the *Bbs*I sites of pUC19_AtU6oligo. Then, the cloned plasmid was digested with restriction enzyme I-SceI, and the gRNA expression cassette was re-cloned into pZD_AtU6gRNA _FFCas9_NPTII. *Agrobacterium tumefaciens* LBA4404 (Takara Bio, Shiga, Japan) was then transformed with the binary vector

Plant transformation and transgenic plant propagation

S. lycopersicum cv. 'Moneymaker' was used for artificial editing by CRISPR/Cas9. Plants were transformed as described by previous study (Sun et al 2006). In brief, diced leaves were inoculated with A. tumefaciens LBA4404 transformed with the constructed binary plasmid vector. Callus was generated, and shoots were formed. The shoots were transferred to and grown on a selective regeneration medium containing 1.5 mg/L zeatin, 50 mg/L kanamycin, and 200 mg/L carbenicillin in a growth chamber (16 h light/8 h dark). Then the largest shoots were transferred to a rooting medium containing 50 mg/L kanamycin, 100 mg/L carbenicillin, and 0.1 mg/L 1-naphthylacetic acid. Lines with roots were transferred for culture in soil pots under white fluorescent light (14 h light/10 h dark). T1 and T2 generations of the transgenic lines were

produced through self-pollination of each parent generation.

Genotyping of Transgenes and Mutations

Tomato genomic DNA was extracted from transgenic and non-transgenic regenerated plants by using a MonoFas Plant DNA Extraction Kit (GL Sciences, Tokyo, Japan). The U6 promoter of the transgene including the gRNA region was checked by polymerase chain reaction (PCR) analysis using a pair of primers (5'-TGGGAATCTGAAAGAAGAGAAGCA-3' and 5'‐AAACGCTGGTATCAGATTTACCCT-3') and KOD-FX enzyme solution (Toyobo, Osaka, Japan). PCR conditions were incubation at 95°C for 2 min, followed by 30 cycles of 98°C for 10s, 55°C for 30s, and 68°C for 20s, with a final step of 68°C for 3 min. Subsequently, the transgenic lines were genotyped for mutations at the DCL3 target sites by using a cleaved amplified polymorphic sequences (CAPS) assay as follows. PCRs were performed under the above conditions, but using a different pair of primers (5'‐CTCAACTATCAAGGCAGCTTG-3' and 5'- CTCCATTAGGATCATTTCCCC-3'), and the PCR products were digested with the restriction enzyme *Hpy*CH4V. The digested products were separated using 1.4% agarose gel electrophoresis. The indel mutations in T1 and T2 progeny seedlings were confirmed by sequencing the target region. PCR fragments from the CAPS assay were cloned into the pGEM-t-easy vector (Promega), and nucleotide sequences of several clones were determined.

Virus inoculation.

Cucumber mosaic virus (CMV^{Y}) inoculations were performed using *in vitro* transcribed full-length viral transcripts as described before (Suzuki et al 1991). Viral infection experiments were repeated at least three times. In every experiment the treatment groups consisted of three plants. The results were highly reproducible and representative data are shown. The protein and RNA

samples, used for northern and western blots, were also prepared and pooled from the three plants, which constituted the given treatment group.

RESULTS

Generation of dcl3-knockout *S. lycopersicum*.

To examine the antiviral role of the DCL3 protein of *S. lycopersicum*, we decided to generate dcl3 mutant plants using the pZD_AtU6gRNA _FFCas9_NPTII. We created a single plasmid system to express the Cas9 protein and the appropriate sgRNA. Tomato DCL3 gene is on chromosomes 8, respectively (Fig 3-1).

Commercial cultivar 'Moneymaker' transformed by *A. tumefaciens* harboring the binary vector for CRISPR-mediated editing of DCL3. The region targeted by the gRNA position showed on the schematic map of DCL3 complete CDS (Figure 3-1). T0 plants were regenerated to evaluate the effectiveness of genome editing at the target sequences.

The CAPS assay for the targeted sites identified 20 transformants with artificially edited DCL3 alleles. T1 progenies were generated from self-pollination of three out of 20 T0 regenerated plants, and generated mutations in the targeted DCL3 loci in their genomes were investigated. DNA fragments including the targeted sites were amplified by PCR and cloned. As a result of nucleotide sequencing of these clones, two types of artificial DCL3 alleles were detected in T1 plants (Figure 3-1), including deletion of two and six nucleotides (2DEL and 6DEL, respectively). Furthermore, null-segregant progenies, without the transgene, were obtained from the T1 or T2 generation. The mutant plants showed almost the same phenotype and traits as WT tomato in the greenhouse cultivation (data not shown).

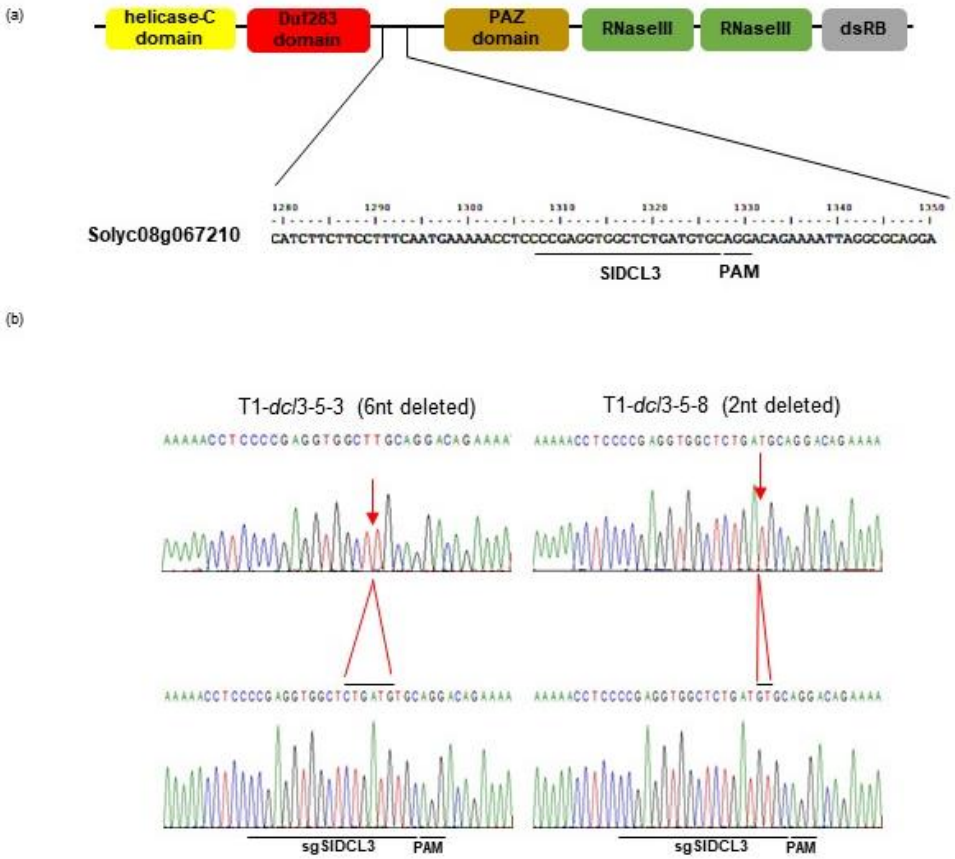

Figure 3-1 Construction for *Solanum lycopersicum* DCL3 knock-out. (a) Gene structure of SlDCL3 showing the gRNA targets. (b) Site-specific mutation positions of SlDCL3 gRNA and PAM sequences are bold and black dashes. Deletion positions are indicated by black dashes in T1 generation.

Dcl3 has a modulatory effect on cucumber mosaic virus infection

Tomato plants were homozygous inoculated for one of the above two artificially edited alleles. CMV-Y strain cause systemic mosaic and yellowing symptoms,

respectively, in tobacco, and CMV after induce systemic mosaic in tomato. At 15 dpi (days-post-inoculation), systemic mosaic symptoms in wild type tomato plants were more severe than those in the plant with the 6EDL alleles (Figure 3-2). In contrast, there were not significant difference in symptoms between 2DEL and WT (Figure 3-2). In a northern and western blot assays, there were significant difference in the viral RNA and CP (coat protein) accumulation.

For viral RNAs, virus-derived small interfering RNAs (vsiRNAs) and coat protein (CP) levels were observed to higher in WT than 6DELs (Figure 3-2) but in 2DEL and WT there was no significant difference in viral RNA, vsiRNA and CP accumulation. These results show that, 6DEL contributes to the tolerance to CMV infection (Figure 3-2).

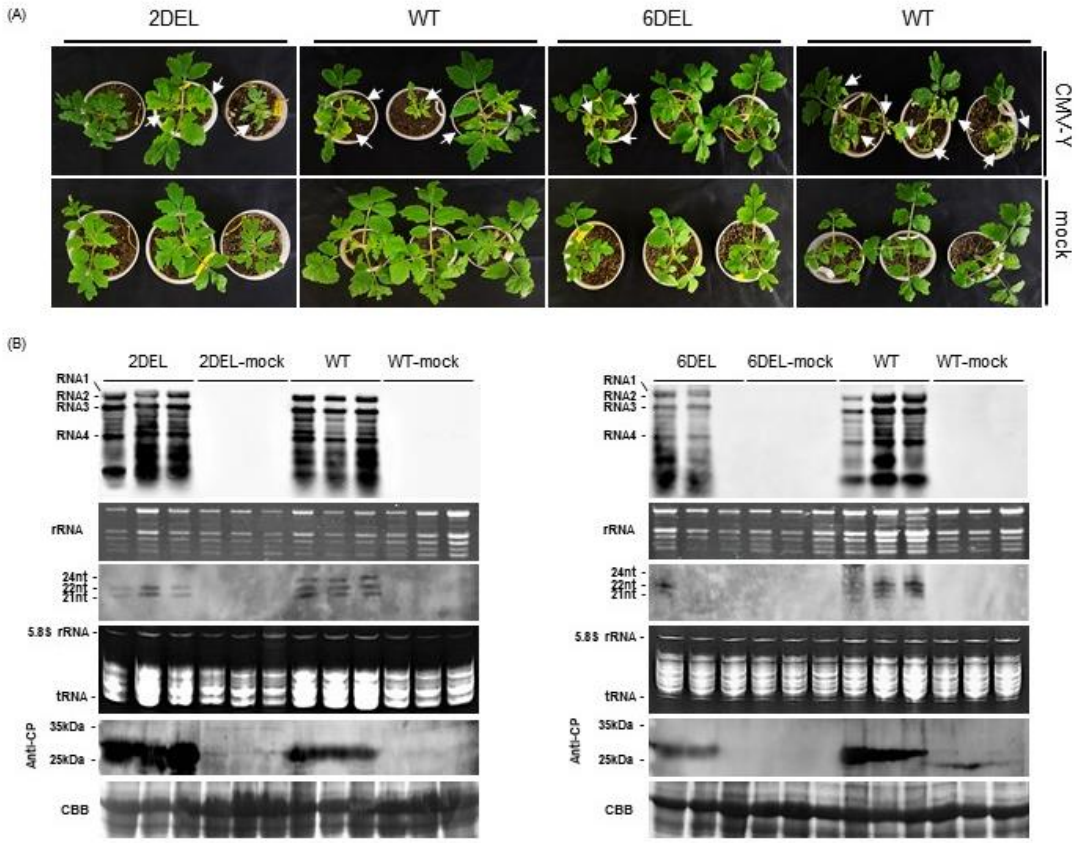

Fig 3-2 Symptoms development and molecular analysis. (A) Symptoms developed in two (2DEL) and six nucleotides deletion (6DEL) knock-out tomato plants inoculated with CMVY. Photographs was captured at 15 days-post-inoculation (dpi). The Moneymaker tomato plants were also inoculated with CMVY (WT) and buffer (Mock) as controls. (B) Detection of genomic RNA, virus derived small interfering RNAs (vsiRNAs) and CMV CP protein in tomato plants inoculated with CMVY using northern and northern blotting. Total RNAs extracted from 2DEL and 6DEL mutants, WT and mock plants at 15 dpi were fractionated using an agarose gel or polyacrylamide gel to detect CMV genomic RNAs (RNA1, 2 and 3), subgenomic RNA4 and vsiRNAs in non-inoculated upper leaves through northern blotting. rRNA and tRNA were used as loading control. Total protein samples were prepared from non-inoculated upper leaves from 2DEL and 6DEL mutants, WT and mock plants at 15 dpi. The CBB-stained gel was used as a loading control (CBB).

DISCUSSION

Programmable DNA cleavage by CRISPR/Cas9 enables targeted inactivation of genes and it also serves as the basis for more sophisticated genome engineering in plants. This system has been demonstrated to work efficiently not only in single cells, but also in whole organisms as well. In genetically intractable species, like the amphidiploid *N. benthamiana*, the use of this technology opens up avenues to generate mutants, which can be used for the genetic dissection of various biological phenomena. Thus, in species like *N. benthamiana* RNAi based methodologies (antisense RNA, VIGS, shRNA) have been available to interrupt the functions of genes of interest. Although widely accepted, skeptics often point out that these techniques suppress gene expression indirectly and the knockdown is often only partial. Additionally, studying components of RNA silencing by using RNAi techniques presents the paradoxical situation, where one relies on the activity of those molecules, which he wishes to disable (Ludman et al 2017). Viral vectors applied for VIGS experiments (TRV, PVX etc.) may also interfere with various endogenous cellular functions and cause unintended changes in the expression of non-target genes, making it difficult to unambiguously interpret the results (Olah et al 2016). This can become especially problematic for studying host-virus interactions, since viruses often exhibit synergistic or antagonistic relationships with each other. Further complicating the issue is that viruses often encode proteins, which can inhibit RNA silencing (VSRs). To circumvent this problem, VSR-deficient forms of viruses are frequently employed. However, the immense amounts of vsiRNAs generally produced during viral infections can themselves saturate and thereby neutralize the silencing effectors.

Therefore, to circumvent the above problems, the CRISPR/Cas9 system was used to generate the dcl3 mutants of *Solanum lycopersicum*. Under the normal growth conditions, the dcl3-6DEL plants did not exhibit any obvious phenotypic alteration. However, dcl3-2DEL had a significant difference of phenotypic alteration compared to wild type tomato (moneymaker). These results

show that the phenotypic alteration of tomatoes is affected in the case of 2-nucleic acid deletion (gene knockout) compared to that of the 6- nucleic acid deletion (2-amino acid inframe).

The lack of dcl3 had differential effects on the plants' antiviral response. 6DEL unexpectedly confers antiviral resistance to CMV but 2DEL did not.

In the previous studies reported that, the lack of the effect of AGO2 on CMV infection is however unexpected, as numerous studies have reported on the sensitizing effect of AGO2 mutation on CMV infection and symptom manifestation in *A. thaliana* (Carbonell A et al 2015, Harvey JJ et al 2011). A possible explanation can be related to the observation that in *N. benthamiana* the down-regulation of RDR6 has aggravated CMV infection (Schwach et al 2005) either suggests that secondary vsiRNAs do not play a critical role in anti-CMV immunity or more likely, other RDRs and/or AGOs (RDR2, AGO1, AGO5 etc.) may have overtaken the above functions of AGO2 and RDR6 in this plant species. Regardless, the knockout of dcl3 gene effect on CMV infection in *S. lycopersicum* emphasizes the need to employ additional model organisms to study host-virus interactions.

In summary, by using the CRISPR/Cas9 system we were able to generate dcl3 mutant line of *S. lycopersicum*, and for the first time provided unequivocal proof for the essential role of DCL3 in antiviral immunity in a plant species. Most viruses are able to efficiently overcome the defense responses of their host plants. Thus, antiviral activities of the components of RNA silencing can usually be studied using mutant viruses, which lack their cognate VSRs. However, VSRs are often multifunctional proteins involved not only in suppressing RNA silencing but in many other aspects of the viral lifecycle. Therefore, their inactivation may result in viruses that are unable to carry out normal infection.

GENERAL DISCUSSION

The tomato (*Solanum lycopersicum*) is the seventh most important crop species and the second-most consumed vegetable in the world (Bergougnoux 2014). An analysis of tomato DCL1 and DCL3-silencing mutants indicates that DCL1 produces canonical miRNAs and a few 21-nt siRNAs (Kravchik et al 2014), and DCL3 is involved in the biosynthesis of heterochromatic 24-nt siRNAs and long miRNAs **(**Kravchik et al 2014**)**. DCL4 is required for the production of 21-nt tasiRNAs that in turn target the ADP-ribosylation factors (ARFs) to alter tomato leaf development (Yifhar et al 2012). A previous study, the full-length cDNA sequences of four tomato DCL2 subfamily members, DCL2a, DCL2b, DCL2c, and DCL2d for a expression pattern analysis, and we showed that the DCL2b expression was much higher than that of other DCL2s, implying its predominant role in biology (Wang et al 2016). DCL2b dependent miRNA pathway in tomato affects susceptibility to PVX and TMV (Wang et al 2018). DCL2b is also required for the biosynthesis of 22-nt small RNAs to defense against ToMV (Wang et al 2018). Based on those previous studies, the role of RNA silencing-related genes in tomato tolerance to viral infection was identified.

In this thesis, RNA silencing-related genes in tomato tolerance to viral infection was examined.

In the chapter one, increased accumulation of PVY CP and genomic RNA with symptoms observed in hpDCL2.4 plants, suggesting that DCL2 and DCL4 are involved in the anti-PVY defense in tomato plants via the RNA silencing mechanism. Although all the PVX-inoculated transgenic plants comparably accumulated CP and genomic RNA, more severe and additional necrotic symptoms were observed in hpDCL2.4 and hpAGO2.3 plants. Based on the present findings, DCL2, DCL4, AGO2 and AGO3 are involved in tolerance to infection with PVX and PVY.

In the chapter two, PVX-inoculated hpAGO2.3 plants showed a consistently higher CP accumulation than wild-type tomato. Furthermore, inoculation tests with chimeric PVX between

strains PVX-UK3 and PVX-8 causes severer necrosis than PVX-UK3. In additionally found that mRNA levels of superoxide dismutase 2 (SOD2) and the copper chaperon for SOD (CCS1), which detoxicates reactive oxygen species (ROS) and are regulated by micro RNAs, decreased in the PVX-infected hpAGO2.3 plants showing necrosis. Taken together, the results indicated that AGO2 and AGO3 would contribute to tomato tolerance to PVX infection by regulating excessive ROS production as well as controlling viral multiplication via RNA silencing mechanism.

In the chapter three, the CRISPR/Cas9 technology to inactivate the DCL3 gene of *S. lycopersicum* to investigated of viral infection. The dcl3 plants exhibit differential sensitivities towards CMV. The result show that, 6DEL unexpectedly confers antiviral resistance to CMV but 2DEL did not. The reason of these antiviral mechanism was not elucidated. Therefore, it is necessary to elucidate this antiviral resistance mechanism by further studies.

Finally, I believe that I could successfully demonstrate three examples of well-organized in roles of RNA silencing-related genes in tomato tolerance to viral infection.

REFERENCES

Achkar NP, Cambiagno DA, Manavella PA. 2016. miRNA biogenesis: a dynamic pathway. Trends In Plant Science 21, 1034–1044.

Aguilar E, Almendral D, Allende L, Pacheco R, Chung BN, Canto T, Tenllado F. 2015. The P25 protein of Potato virus X (PVX) is the main pathogenicity determinant responsible for systemic necrosis in PVX-associated synergisms. Journal of Virology 89, 2090-2103.

Andika IB, Maruyama K, Sun L, Kondo H, Tamada T, Suzuki N. 2015. Differential contributions of plant Dicer-like proteins to antiviral defences against potato virus X in leaves and roots. The Plant Journal 81, 781–93.

Andika IB, Maruyama K, Sun L, Kondo H, Tamada T, Suzuki N. 2015. Different Dicer-like protein components required for intracellular and systemic antiviral silencing in *Arabidopsis thaliana*. Plant Signal and Behavior 10, e1039214.

Angel CA, Schoelz JE. 2013. A survey of resistance to Tomato bushy stunt virus in the genus Nicotiana reveals that the hypersensitive response is triggered by one of three different viral proteins. Molecular Plant Microbe Interactions 26, 240 –248.

Bai M, Yang GS, Chen WT, Mao ZC, Kang HX, Chen GH, Yang YH, Xie BY. 2012. Genome-wide identification of Dicer-like, Argonaute and RNA-dependent RNA polymerase gene families and their expression analyses in response to viral infection and abiotic stresses in *Solanum lycopersicum*. Gene 501, 52-62.

Barrangou R, Doudna JA. 2016. Applications of CRISPR technologies in research and beyond. Nature Biotechnology 34, 933–941.

Baulcombe D. 2004. RNA silencing in plants. Nature 431, 356–363.

Beauclair L, Yu A, Bouché N. 2010. microRNA-directed cleavage and translational repression of the copper chaperone for superoxide dismutase mRNA in Arabidopsis. The Plant Journal 62, 454–462.

Bergougnoux, Véronique. 2014. The history of tomato: from domestication to biopharming. Biotechnology Advances 32, 170-89.

Blevins T, Podicheti R, Mishra V, Marasco M, Wang J, Rusch D, Tang H, Pikaard CS. 2015. Identification of Pol IV and RDR2-dependent precursors of 24nt siRNAs guiding de novo DNA methylation in Arabidopsis. eLife 4, e9591.

Brosseau C, Moffett P. 2015. Functional and genetic analysis identify a role for Arabidopsis ARGONAUTE5 in antiviral RNA silencing. Plant Cell 27, 1742–54.

Calarco JP, Martienssen, RA. 2011. Genome reprogramming and small interfering RNA in the *Arabidopsis* germline. Current Opinion in Genetic and Development 21, 134–9.

Carbonell A, Carrington JC. 2015. Antiviral roles of plant ARGONAUTES. Current Opinion in Genetic and Development 27, 111–7.

Carthew RW, Sontheimer EJ. 2009. Origins and Mechanisms of miRNAs and siRNAs. Cell 136, 642–655.

Chapman S, Kavanagh T, Baulcombe DC. Potato virus X as a vector for gene expression in plants. The Plant Journal 2, 549–57.

Chen H, Chen L, Patel K, Li Y, Baulcombe DC, Wu S. 2010. 22-nucleotide RNAs trigger secondary siRNA biogenesis in plants. Proceedings of The National Academy of Sciences 107, 15269–15274.

Cuperus JT, Carbonell A, Fahlgren N, Garcia-ruiz H, Burke RT, Takeda A, Sullivan CM, Gilbert SD, Montgomery TA, Carrington JC. 2010. Unique functionality of 22-nt miRNAs

in triggering RDR6-dependent siRNA biogenesis from target transcripts in Arabidopsis. Nature Structural and Molecular Biology 17, 997–1004.

Zhang K, Raboanatahiry N, Zhu B, Li M. 2017 Progress in genome editing technology and its application in plants. Frontier in Plant Science 8, 177.

Chen X. 2010. Small RNAs – secrets and surprises of the genome. Plant Journal. 61, 941–58.

Cho SK, Ryu MY, Shah P, Poulsen CP, Yang SW. 2016. Post-Translational Regulation of miRNA Pathway Components, AGO1 and HYL1, in Plants. Molecular Cells 39, 581.

Chung BYW, Miller WA, Atkins JF, Firth AE. 2008. An overlapping essential gene in the Potyviridae. Proceedings of The National Academy of Sciences USA 105, 5897–902.

Cogoni C, Macino G. 1999. Gene silencing in *Neurospora crassa* requires a protein homologous to RNA-dependent RNA polymerase. Nature 399, 166–9.

Cong L, Ran FA, Cox D, Lin S, Barretto R, Habib N, Hsu PD, Wu X, Jiang W, Marraffini LA, Zhang F. 2013. Multiplex genome engineering using CRISPR/Cas9 systems. Science 339, 819–823.

Cordero T, Cerdán L, Carbonell A, Katsarou K, Kalantidis K, Daròs JA. 2017. Dicer-Like 4 Is Involved in Restricting the Systemic Movement of *Zucchini yellow mosaic virus* in *Nicotiana benthamiana*. Molecular Plant Microbe Interaction 30, 63–71.

Csorba T, Pantaleo, V, Burgyán J. 2009. RNA silencing: an antiviral mechanism. In Loebenstein G, Carr JP, editors. Adv Virus Res. London: Academic Press p. 35-230.

Dalmay T, Hamilton A, Rudd S, Angell S, Baulcombe DC. 2000. An RNA-dependent RNA polymerase gene in *Arabidopsis* is required for posttranscriptional gene silencing mediated by a transgene but not by a virus. Cell 101, 543–53.

De S, Chavez-Calvillo G, Wahlsten M, Mäkinen K. 2018. Disruption of the methionine cycle and reduced cellular gluthathione levels underlie potex– potyvirus synergism in *Nicotiana benthamiana*. Molecular Plant Pathology 19, 1820-1835.

Deleris A, Gallego-Bartolome J, Bao J, Kasschau KD, Carrington JC, Voinnet O. 2006. Hierarchical action and inhibition of plant Dicer-like proteins in antiviral defense. Science 313, 68–71.

Diaz-Pendon J. A, Li F, Li WX, Ding SW. 2007. Suppression of antiviral silencing by cucumber mosaic virus 2b protein in *Arabidopsi*s is associated with drastically reduced accumulation of three classes of viral small interfering RNAs. Plant Cell. 19, 2053–63.

Ding SW, Voinnet O. 2017. Antiviral immunity directed by small RNAs. Cell 130, 413426.

Ding SW. 2010. RNA-based antiviral immunity. Nature Reviews Immunology 10, 632–644.

Doke N. 1983. Generation of superoxide anion by potato tuber protoplasts during hypersensitive response to hyphal wall components of *Phytophtora infestans* and specific inhibition of the reaction with supressors of hypersensitivity. Physiological Plant Pathology 23, 359-367.

Doudna JA, Charpentier E. 2014. Genome editing. The new frontier of genome engineering with CRISPR-Cas9. Science 346, 1258096–1258096.

Dunoyer P, Himber C, Ruiz-Ferrer V, Alioua A, Voinnet O. 2007. Intra- and intercellular RNA interference in *Arabidopsis thaliana* requires components of the microRNA and heterochromatic silencing pathways. Nature Genetics 39, 848–56.

Fátyol K, Fekete KA, Ludman M. 2020. Double-Stranded-RNA-Binding Protein 2 Participates in Antiviral Defense. Journal of Virology 94, 11.

Feng K, Yu J, Cheng Y, Ruan M, Wang R, Ye Q, Zhou G, Li Z, Yao Z, Yang Y, Zheng Q, Wan H. 2016. The SOD gene family in tomato: identification, phylogenetic relationships, and expression patterns. Frontier in Plant Science 7, 1279.

Fernández-Calvino L, Martínez-Priego L, Szabo EZ, Guzmán-Benito I, González I, Canto T, Lakatos L, Llave C. 2016. Tobacco rattle virus 16K silencing suppressor binds ARGONAUTE 4 and inhibits formation of RNA silencing complexes. Journal of General Virology 97, 246–57.

Fukudome A, Fukuhara T. 2017. Plant dicer-like proteins: double-stranded RNAcleaving enzymes for small RNA biogenesis. Journal of Plant Research 130, 33–44.

García-Marcos A, Pacheco R, Manzano A, Aguilar E, Tenllado F. 2013. Oxylipin biosynthesis genes positively regulate programmed cell death during compatible infections with the synergistic pair Potato virus X-Potato virus Y and Tomato spotted wilt virus. Journal of Virology 87, 5769-5783.

García-Marcos A, Pacheco R, Martiáñez J, González-Jara P, Díaz-Ruíz JR, Tenllado F. 2009. Transcriptional changes and oxidative stress associated with the synergistic interaction between Potato virus X and Potato virus Y and their relationship with symptom expression. Molecular Plant Microbe Interactions 22, 1431-1444.

Garcia-Ruiz H, Carbonell A, Hoyer JS, Fahlgren N, Gilbert KB, Takeda A, Giampetruzzi A, Garcia Ruiz MT, McGinn MG, Lowery N, Martinez Baladejo MT, Carrington JC. 2015. Roles and programming of Arabidopsis ARGONAUTE proteins during Turnip Mosaic Virus infection. Plos Pathogens 11, e1004755.

Garcia-Ruiz H, Takeda A, Chapman EJ, Sullivan CM, Fahlgren N, Brempelis KJ, Carrington JC. 2010. *Arabidopsis* RNA-Dependent RNA Polymerases and Dicer-Like Proteins in Antiviral Defense and Small Interfering RNA Biogenesis during *Turnip Mosaic Virus* Infection. Plant Cell 22, 481–96.

Gallitelli D, Di Franco A, Vovlas C, Kaper JM. 1988. Infezioni miste del virus del mosaico del cetriolo (CMV) e di potyvirus in colture ortive di Puglia e Basilicata. Informatore Fitopatologico 12, 57–64.

González-Jara P, Atencio FA, Martínez-García B, Barajas D, Tenllado F, Díaz-Ruíz JR. 2005. A single amino acid mutation in the Plum pox virus helper component-proteinase gene abolishes both synergistic and RNA silencing suppression activities. Phytopathology 95, 894-901.

González-Jara P, Tenllado F, Martínez-García B, Atencio FA, Barajas D, Vargas M, DíAZ-RUIZ J, Díaz-Ruíz, JR. 2004. Host-dependent differences during synergistic infection by Potyviruses with potato virus X. Molecular Plant Pathology 5, 29-35.

Grant-Downton R, Kourmpetli S, Hafidh S, Khatab H, Le Trionnaire G, Dickinson H, Twell D. 2013 Artificial microRNAs reveal cell-specific differences in small RNA activity in pollen. Current Biology 23, 599–601.

Harrison MM., Jenkins BV, O'Connor-Giles KM, Wildonger JA. 2014. CRISPR view of development. Genes and Development 28, 1859–1872.

Harvey JJ, Lewsey MG, Patel K, Westwood J, Heimstädt S, Carr JP, Baulcombe DC. 2011. An Antiviral Defense Role of AGO2 in plants. Plos One 6, e14639.

Hochstrasser ML, Doudna, JA. 2015. Cutting it close: CRISPR-associated endoribonuclease structure and function. Trends in Biochemical Sciences 40, 58–66.

Holoch D. Moazed D. 2015. RNA-mediated epigenetic regulation of gene expression. Nature Reviews Genetics 16, 71–84.

Jaubert M, Bhattacharjee S, Mello AF, Perry KL, Moffett P. 2011. ARGONAUTE2 Mediates RNA-Silencing Antiviral Defenses against *Potato virus X* in Arabidopsis. Plant Physiology 156, 1556–64.

Jeon EJ, Tadamura K, Murakami T, Inaba JI, Kim BM, Sato M, Nakahara KS. 2017. rgs-CaM Detects and Counteracts Viral RNA Silencing Suppressors in Plant Immune Priming. Journal of Virology 91, 19.

Jinek M, Chylinski K, Fonfara I, Hauer M, Doudna JA, Charpentier E. 2012. A programmable dual-RNA-guided DNA endonuclease in adaptive bacterial immunity. Science 337, 816–821,

Jones L, Hamilton AJ, Voinnet O, Thomas CL, Maule AJ, Baulcombe DC. 1999. RNA–DNA interactions and DNA methylation in post-transcriptional gene silencing. The Plant Cell 11, 2291-2301.

Juszczak I, Baier M. 2012. The strength of the miR398-Csd2-CCS1 regulon is subject to natural variation in *Arabidopsis thaliana*. FEBS Letters 586, 3385–3390.

Kagiwada S, Yamaji Y, Komatsu K, Takahashi S, Mori T, Hirata H, Suzuki M, Ugaki M, Namba S. 2005. A single amino acid residue of RNA-dependent RNA polymerase in the Potato virus X genome determines the symptoms in *Nicotiana* plants. Virus Research. 110, 177-182.

Karasev A. V, Gray SM. 2013. Continuous and Emerging Challenges of *Potato virus Y* in Potato. Annual Review of Phytopathology 51, 571–86.

Király L, Cole AB, Bourque JE, Schoelz JE. 1999. Systemic cell death is elicited by the interaction of a single gene in *Nicotiana clevelandii* and gene VI of Cauliflower mosaic virus. Molecular Plant Microbe Interactions 12, 919-925.

Komatsu K, Hashimoto M, Ozeki J, Yamaji Y, aejima K, enshu H, Himeno M, Okano Y, Kagiwada S, Namba S. 2010. Viral-induced systemic necrosis in plants involves both programmed cell death and the inhibition of viral multiplication, which are regulated by independent pathways. Molecular Plant Microbe Interactions 23, 283-293.

Komoda YH, Choi SH, Sato M, Atsumi G, Abe J, Fukuda J, Honjo MN, Nagano AJ, Komoda, Nakahara KS, Uyeda I. 2016. Truncated yet functional viral protein produced *via* RNA polymerase slippage implies underestimated coding capacity of RNA viruses. Scientific Reports UK 6, 21411.

Kravchik M, Damodharan S, Stav R, Arazi T. 2014. Characterization of a tomato DCL3-silencing mutant. Plant Science 221, 81-89.

Kravchik M, Sunkar R, Damodharan S, Stav R, Zohar M, Isaacson T, Arazi T. 2014 Global and local perturbation of the tomato microRNA pathway by a trans-activated DICER-LIKE 1 mutant. Journal of Experiment Botany 65, 725–739.

Kwon J, Kasai A, Maoka T, Masuta C, Sano T, Nakahara KS. 2020. RNA silencing-related genes contribute to tolerance of infection with potato virus X and Y in a susceptible tomato plant. Virology Journal 17, 1-13.

Lamb C, Dixon RA. 1997. The oxidative burst in plant disease resistance. Annual Review of Plant Biology 48, 251-275.

Li F, Pignatta D, Bendix C, Brunkard JO, Cohn MM, Tung J, Sun H. 2011.MicroRNA regulation of plant innate immune receptors. Proceedings of The National Academy of Sciences 109, 1790–1795.

Li JF, Chung HS, Niu Y, Bush J, McCormack M, Sheen J. 2013 Comprehensive protein-based artificial microRNA screens for effective gene silencing in plants. Plant Cell 25, 1507–1522.

Li S, Liu L, Zhuang X, Yu Y, Liu X, Cui X, Ji L, Pan Z, Cao X, Mo B, Zhang F, Raikhel N, Jiang L, Chen X. 2013 MicroRNAs inhibit the translation of target mRNAs on the endoplasmic reticulum in Arabidopsis. Cell 153, 562–574.

Li S, Castillo-Gonzalez C, Yu B, Zhang X. 2017. The functions of plant small RNAs in development and in stress responses. The Plant Journal 90, 654–670.

Love AJ, Laird J, Holt J, Hamilton AJ, Sadanandom A, Milner JJ. 2007. Cauliflower mosaic virus protein P6 is a suppressor of RNA silencing. Journal of General Virology 88, 3439 –3444.

Lu Y, Yin M, Wang X, Chen B, Yang X, Peng J, MacFarlane S. 2016. The unfolded protein response and programmed cell death are induced by expression of Garlic virus X p11 in *Nicotiana benthamiana*. Journal of General Virology 97, 1462–8.

Ludman M, Burgyán J, Fátyol K. 2017. Crispr/Cas9 mediated inactivation of Argonaute 2 reveals its differential involvement in antiviral responses. Scientific Reports 7, 1-12.

Ma X, Nicole MC, Meteignier L. V, Hong N, Wang G, Moffett P. 2015. Different roles for RNA silencing and RNA processing components in virus recovery and virus-induced gene silencing in plants. Journal of Experimental Botany 66, 919–32.

Mahjabeen, Akhtar KP, Sarwar N, Saleem MY, Asghar M, Iqbal Q, Jamil, FF. 2012. Effect of cucumber mosaic virus infection on morphology, yield and phenolic contents of tomato. Phytopathology 45, 766–782.

Malcuit I, Marano MR, Kavanagh TA, De Jong W, Forsyth A, Baulcombe DC. 1999. The 25-kDa Movement Protein of PVX Elicits *Nb*-Mediated Hypersensitive Cell Death in Potato. Molecular Plant Microbe Interactions 12, 536–43.

Mali P, Yang L, Esvelt KM, Aach J, Guell M, DiCarlo JE, Norville JE, Churc GM. 2013. A-guided human genome engineering via Cas9. Science 339, 823–826

Mandadi KK, Scholthof KB. 2013. Plant immune responses against viruses: how does a virus cause disease? Plant Cell 25, 1489 –1505.

Martinez de Alba AE, Elvira-Matelot E, Vaucheret H. 2013. Gene silencing in plants: a diversity of pathways. Biochim Biophys Acta 1829, 1300–1308.

Masuta C, Nishimura M, Morishita H, Hataya T. 1999. A Single Amino Acid Change in Viral Genome-Associated Protein of Potato Virus Y Correlates with Resistance Breaking in 'Virgin A Mutant' Tobacco. Phytopathology 89, 118–23.

Matsuo K, Matsumura T. 2017. Repression of the DCL2 and DCL4 genes in *Nicotiana benthamiana* plants for the transient expression of recombinant proteins. Journal of Bioscience and Bioengineering 124, 215-20.

Mikami M., Toki S, Endo M. 2015. Comparison of CRISPR/Cas9 expression constructs for efficient targeted mutagenesis in rice. Plant Molecular Biology 88, 561–572.

Kanazashi Y, Hirose A, Takahashi I, Mikami M, Endo M, Hirose S, Toki S, Kaga A, Naito K, Ishimoto M, Abe J, Yamada T. 2018. Simultaneous site-directed mutagenesis of duplicated loci in soybean by using a single guide RNA. Plant Cell Reports 37, 553–563.

Miller G, Suzuki N, Ciftci-Yilmaz S, Mittler R. 2010. Reactive oxygen species homeostasis and signalling during drought and salinity stresses. Plant Cell Environ 33, 453-467

Minoia S, Carbonell A, Di Serio F, Gisel A, Carrington JC, Navarro B, Flores, R. 2014. Specific argonautes selectively bind small RNAs derived from Potato Spindle Tuber Viroid and Attenuate Viroid accumulation *in vivo*. Journal of Virology 88, 11933–11945.

Mittler R, Vanderauwera S, Gollery M, Van Breusegem F. 2004. Reactive oxygen gene network of plants. Trends Plant Science. 9, 490-498.

Nakahara KS, Masuta C, Yamada S, Shimura H, Kashihara Y, Wada TS, Sekiguchi T. 2012. Tobacco calmodulin-like protein provides secondary defense by binding to and directing degradation of virus RNA silencing suppressors. Proceedings of the National Academy of Sciences 109, 10113-10118.

Naoi T, Kitabayashi S, Kasai A, Sugawara K, Adkar-Purushothama CR, Senda M, Hataya T, Sano T. 2020. Suppression of RNA-dependent RNA polymerase 6 in tomatoes allows potato

spindle tuber viroid to invade basal part but not apical part including pluripotent stem cells of shoot apical meristem. Plos One 15, e0236481

Odokonyero D, Mendoza M. R, Alvarado VY, Zhang J, Wang X, Scholthof HB. 2015. Transgenic down-regulation of ARGONAUTE2 expression in *Nicotiana benthamiana* interferes with several layers of antiviral defenses. Virology 486, 209–18.

Ohki T, Sano M, Asano K, Nakayama T, Maoka T. 2018. Effect of temperature on resistance to *Potato virus Y* in potato cultivars carrying the resistance gene Ry_{chc}. Plant Pathology 67, 1629–35.

Olspert A, Chung BYW, Atkins JF, Carr JP, Firth AE. 2015. Transcriptional slippage in the positive-sense RNA virus family *Potyviridae*. EMBO Reports. 16, 995–1004.

Olah E, Pesti R, Taller D, Havelda Z, Varallyay E. 2016. Non-targeted effects of virus-induced gene silencing vectors on host endogenous gene expression. Archives of Virology 161, 2387–2393.

Osmani Z, Jin S, Mikami M, Endo M, Atarashi H, Fujino K, Yamada T. 2019. CRISPR/Cas9-mediated editing of genes encoding rgs-CaM-like proteins in transgenic potato plants. Methods in Molecular Biology 2028, 153–165.

Ozeki J, Takahashi S, Komatsu K, Kagiwada S, Yamashita K, Mori T, Namba S. 2006. A single amino acid in the RNA-dependent RNA polymerase of Plantago asiatica mosaic virus contributes to systemic necrosis. Archives of Virology 151, 2067–75.

Pacheco R, García-Marcos A, Barajas D, Martiáñez J, Tenllado F. 2012. PVX–potyvirus synergistic infections differentially alter microRNA accumulation in *Nicotiana benthamiana*. Virus Research 165, 231–5.

Plisson C, Drucker M, Blanc S, German-Retana S, Le Gall O, Thomas D, Bron P. 2003. Structural Characterization of HC-Pro, a Plant Virus Multifunctional Protein. Journal of Biological Chemistry 278, 23753–61.

Pruss G, Ge X, Shi XM, Carrington JC, Vance VB. 1997. Plant viral synergism: the potyviral genome encodes a broad-range pathogenicity enhancer that transactivates replication of heterologous viruses. The Plant Cell 9, 859-868.

Qu F, Ye X, Morris TJ. 2008. *Arabidopsis* DRB4, AGO1, AGO7, and RDR6 participate in a DCL4-initiated antiviral RNA silencing pathway negatively regulated by DCL1. Proceedings of The National Academy of Sciences USA 105, 14732–7.

Riechmann JL, Laín S, García JA. 1992. Highlights and prospects of potyvirus molecular biology. Journal of General Virology 73, 1–16.

Ruiz-Ferrer V, Voinnet O. 2009. Roles of plant small RNAs in biotic stress responses. Annual Review of Plant Biology 60, 485-510.

Scholthof HB, Alvarado VY, Vega-Arreguin JC, Ciomperlik J, Odokonyero D, Brosseau C, Jaubert M, Zamora A, Moffett P. 2015. Identification of an ARGONAUTE for antiviral RNA silencing in *Nicotiana benthamiana.* Plant Physiology 156, 1548–55.

Schuck J, Gursinsky T, Pantaleo V, Burgy´an,J, Behrens SE. 2013. AGO/RISC-mediated antiviral RNA silencing in a plant *in vitro* system. Nucleic Acids Research 41, 5090–103.

Schwach F, Vaistij FE, Jones L, Baulcombe DC. 2005. An RNA-dependent RNA polymerase prevents meristem invasion by potato virus X and is required for the activity but not the production of a systemic silencing signal. Plant Physiology 138, 1842–1852.

Senshu H, Ozeki J, Komatsu K, Hashimoto M, Hatada K, Aoyama M, Namba S. 2009. Variability in the level of RNA silencing suppression caused by triple gene block protein 1

(TGBp1) from various potexviruses during infection. Journal of General Virology 90, 1014–24.

Song X, Li P, Zhai J, Zhou M, Ma L, Liu B, Jeong DH, Nakano M, Cao S, Liu C, Chu C, Wang XJ, Green PJ, Meyers BC, Cao X. 2012. Roles of DCL4 and DCL3b in rice phased small RNA biogenesis. Plant Journal 69, 462–474.

Sun HJ, Uchii, S Watanabe S, Ezura H. 2006. A highly efficient transformation protocol for micro-tom, a model cultivar for tomato functional genomics. Plant Cell Physiology 47, 426–431.

Sunkar R, Kapoor A, Zhu JK. 2006. Posttranscriptional induction of two Cu/Zn superoxide dismutase genes in Arabidopsis is mediated by downregulation of miR398 and important for oxidative stress tolerance. The Plant Cell 18, 2051-2065.

Suzuki M, Kuwata S, Kataoka J, Masuta C, Nitta N, Takanami, Y. 1991. Functional analysis of deletion mutants of cucumber mosaic virus RNA3 using an in vitro transcription system. Virology 183, 106-113.,

Suzuki T, Ikeda S, Kasai A, Taneda A, Fujibayashi M, Sugawara K, Okuta M, Maeda H, Sano T. 2019. RNAi-mediated down-regulation of Dicer-Like 2 and 4 changes the response of 'Moneymaker' tomato to potato spindle tuber viroid infection from tolerance to lethal systemic necrosis, accompanied by up-regulation of miR398, 398a-3p and production of excessive amount of reactive oxygen species. Viruses 11, 344.

Syller J. 2012. Facilitative and antagonistic interactions between plant viruses in mixed infections. Molecular Plant Pathology 13, 204-216.

Takeda A, Iwasaki S, Watanabe T, Utsumi M, Watanabe Y. 2008. The mechanism selecting the guide strand from small RNA duplexes is different among *Argonaute* proteins. Plant Cell Physiology 49, 493–500.

Taochy C, Gursanscky NR, Cao J, Fletcher SJ, Dressel U, Mitter N, Tucker MR, Koltunow A, Bowman JL, Vaucheret H, Carroll BJ. 2017. A genetic screen for impaired systemic RNAi highlights the crucial role of DICER-LIKE 2. Plant Physiology 175, 1424–1437.

Van Wezel R, Hong Y. 2004. Virus survival of RNA silencing without deploying protein-mediated suppression in *Nicotiana benthamiana*. FEBS Letters 562, 65–70.

Vance VB, Berger PH, Carrington JC, Hunt AG, Shi XM. 1995. 5'-proximal potyviral sequences mediate potato virus X/potyviral synergistic disease in transgenic tobacco. Virology 206, 583-590.

Vance VB. 1991. Replication of potato virus X RNA is altered in coinfections with potato virus Y. Virology 182, 486-494.

Vazquez F. 2006. *Arabidopsis* endogenous small RNAs: highways and byways. Trends in Plant Science 11, 460–8.

Verchot-Lubicz J, Ye CM, Bamunusinghe D. 2017. Molecular biology of potexviruses: recent advances. Journal of General Virology 88, 1643–55.

Voinnet O, Lederer C, Baulcombe DC. 2000. A Viral Movement Protein Prevents Spread of the Gene Silencing Signal in *Nicotiana benthamiana*. Cell 103, 157–67.

Voinnet O. 2009. Origin, biogenesis, and activity of plant microRNAs. Cell 136, 669–687

Wang H, La Russa M, Qi LS. 2016. CRISPR/Cas9 in Genome Editing and Beyond. Annual Review of Biochemistry 85, 227–264.

Wang T, Deng Z, Zhang X, Wang H, Wang Y, Liu X, Liu S, Xu F, Li T, Fu D, Shu B, Luo Y, Zhu H. 2018. Tomato DCL2b is required for the biosynthesis of 22-nt small RNAs, the resulting secondary siRNAs, and the host defense against ToMV. Horticultural Research 5, 1-14.

Wang XB, Jovel J, Udomporn P, Wang Y, Wu Q, Li WX, Gasciolli V, Vaucheret H, Ding SW. 2011. The 21-nucleotide, but not 22-nucleotide, viral secondary small interfering RNAs direct potent antiviral defense by two cooperative Argonautes in *Arabidopsis thaliana.* Plant Cell 23, 1625–38.

Wang XB, Wu Q, Ito T, Cillo F, Li WX, Chen X, Yu JL, Ding SW. 2010. RNAi-mediated viral immunity requires amplification of virus-derived siRNAs in *Arabidopsis thaliana*. Proceedings of The National Academy of Sciences USA 107, 484–9.

Wang Z, Hardcastle TJ, Pastor, AC, Yip WH, Tang S, Baulcombe DC. 2018. A novel DCL2-dependent miRNA pathway in tomato affects susceptibility to RNA viruses. Genes and Development 32, 1155-60.

Wilson RC, Doudna JA. 2013. Molecular mechanisms of RNA interference. Annual Review of Biophysics 42, 217–239.

Wong SM, Mahtani PH, Lee KC, Yu HH, Tan Y, Neo KK, Chang NY, Wu M, Chng CG. 1997. Cymbidium mosaic potexvirus RNA: complete nucleotide sequence and phylogenetic analysis. Archives of Virology 142, 383-391.

Wu Y, Hou BH, Lee WC, Lu SH, Yang CJ, Vaucheret H, Chen HM. 2017. DCL2-and RDR6-dependent transitive silencing of SMXL4 and SMXL5 in Arabidopsis dcl4 mutants causes defective phloem transport and carbohydrate over-accumulation. The Plant Journal 90, 1064–1078.

Wylie SJ, Adams M, Chalam C, Kreuze J, López-Moya JJ, Ohshima K, Zerbini F M. 2017. ICTV virus taxonomy profile: *Potyviridae*. Journal of General Virology 98, 352.

Xia C, Li S, Hou W, Fan Z, Xiao H, Lu M., Sano T, Zhang Z. 2017 Global transcriptomic changes induced by infection of cucumber (*Cucumis sativus* L.) with mild and severe variants of hop stunt viroid. Frontier Microbiology 8, 2427.

Xie Z, Johansen LK, Gustafson AM, Kasschau KD, Lellis AD, Zilberman D, Jacobsen SE, Carrington JC. 2004. Genetic and functional diversification of small RNA pathways in plants. Plos Biology 2, e104.

Bouché N, Lauressergues D, Gasciolli V, Vaucheret H. 2006. An antagonistic function for *Arabidopsis* DCL2 in development and a new function for DCL4 in generating viral siRNAs. EMBO Journal 25, 3347–56.

Ye C, Dickman MB, Whitham SA, Payton M, Verchot J. 2011. The Unfolded Protein Response is Triggered by a Plant Viral Movement Protein. Plant Physiology 156, 741–55.

Yifhar T, Pekker I, Peled D, Friedlander G, Pistunov A, Sabban M, Wachsman G, Alvarez JP, Amsellem Z, Eshed Y. 2012. Failure of the tomato trans-acting short interfering RNA program to regulate AUXIN RESPONSE FACTOR3 and ARF4 underlies the wiry leaf syndrome. Plant Cell 24, 3575–3589.

Zhang C, Wu Z, Li Y, Wu J. 2015. Biogenesis, function, and applications of virus-derived small RNAs in plants. Frontier Microbiology 6, 1237.

Zheng Y, Wang Y, Ding B, Fei Z. 2017 Comprehensive transcriptome analyses reveal that potato spindle tuber viroid triggers genome-wide changes in alternative splicing, inducible trans-acting activity of phased secondary small interfering RNAs, and immune responses. Jouranl of Virology 91, e00247-17.

Zhu H, Zhou Y, Castillo-Gonzál C, Lu A, Ge C, Zhao YT, Duan L, Li Z, Axtell MJ, Wang XJ, Zhang X. 2013 Bidirectional processing of pri-miRNAs with branched terminal loops by Arabidopsis Dicer-like1. Nature Structural and Molecular Biology 20, 1106.

ACKNOWLEDGEMENT

I sincerely express my gratitude to my supervisor, Professor Kenji Nakahara, Pathogen-Plant Interaction Laboratory, Hokkaido University for his unstinted support. His infinite passion on research, style of student supervision and kind words, always motivated me to become a scientist like him.

I also truly grateful to Prof 'Masuta Chikara', Pathogen-Plant Interaction Laboratory, Hokkaido University for his kind advice and assistance rendered me during this period.

I specially thank to PhD candidates ‘Takashi Naoi’ from his advised for experiment and lab lifes and being a colleague and a friend during 3 years. And also, thanks for helping in lab life to Dr 'Hangil Kim' and PhD partner 'Jae cheol Shim'.

Further, I would like to extend my sincere thanks to all my labmates at Pathogen-Plant Interaction Laboratory, who extended their support whenever I needed.

I always thanks to my parents for supporting everything in my life and also, truly grateful Prof Jin Sung Hong in Kangwon National University for supporting during the study in Japan.

홋카이도 대학 병원체 식물 상호 작용 연구소의 Kenji Nakahara 교수님의 변함없는 지원에 진심으로 감사드립니다.

연구에 대한 그의 무한한 열정, 학생 감독 스타일 및 그의 친절한 조언은 항상 그와 같은 과학자가 되도록 저에게 동기를 부여했습니다.

또한이 기간 동안 저에게 주신 친절한 조언과 도움에 대해 홋카이도 대학 병원체-식물 상호 작용 연구소의 'Matsuta Chikara'교수에게 진심으로 감사드립니다.

특히 처음 이곳에 와서 졸업까지 3 년동안 저의 실험에 대한 조언 및 일본에서 생활에 대한 큰 도움을 준 박사 후보자 'Takashi Naoi ' 에게 감사드립니다.

또한 같은 한국인 유학생인 출신인 김한길 박사님과 친구이자 같은 유학동기인 재철이에게도 3 년동안 저에게 도움을 주셔서 진심으로 감사합니다.

또한 필요할 때마다 지원을 해주신 병원체-식물 상호 작용 연구소의 모든 연구실 동료들에게 진심으로 감사의 말씀을 드리며 모두들 부디 졸업후에 하고싶은 일을 할 수 있도록 소원합니다.

항상 제 삶의 모든 것을 지원해주신 부모님과 일본 유학을 지원해주신 강원대학교 홍진성 교수님께 진심으로 감사의 말씀을 드립니다.